



HAL
open science

Sequential or simultaneous injection of preformed fibrils and AAV overexpression of alpha-synuclein are equipotent in producing relevant pathology and behavioral deficits

Matilde Negrini, Giuseppe Tomasello, Marcus Davidsson, Alexis Fenyi, Cécile Adant, Swantje Hauser, Elena Espa, Francesco Gubinelli, Fredric Manfredsson, Ronald Melki, et al.

► To cite this version:

Matilde Negrini, Giuseppe Tomasello, Marcus Davidsson, Alexis Fenyi, Cécile Adant, et al.. Sequential or simultaneous injection of preformed fibrils and AAV overexpression of alpha-synuclein are equipotent in producing relevant pathology and behavioral deficits. *Journal of Parkinson's disease*, 2022, 12, pp.1133 - 1153. 10.3233/jpd-212555 . cea-03683739

HAL Id: cea-03683739

<https://cea.hal.science/cea-03683739>

Submitted on 31 May 2022

HAL is a multi-disciplinary open access archive for the deposit and dissemination of scientific research documents, whether they are published or not. The documents may come from teaching and research institutions in France or abroad, or from public or private research centers.

L'archive ouverte pluridisciplinaire **HAL**, est destinée au dépôt et à la diffusion de documents scientifiques de niveau recherche, publiés ou non, émanant des établissements d'enseignement et de recherche français ou étrangers, des laboratoires publics ou privés.



Distributed under a Creative Commons Attribution - NonCommercial 4.0 International License

Research Report

Sequential or Simultaneous Injection of Preformed Fibrils and AAV Overexpression of Alpha-Synuclein Are Equipotent in Producing Relevant Pathology and Behavioral Deficits

Matilde Negrini^a, Giuseppe Tomasello^a, Marcus Davidsson^{b,c}, Alexis Fenyi^d, Cecile Adant^a, Swantje Hauser^a, Elena Espa^c, Francesco Gubinelli^a, Fredric P. Manfredsson^b, Ronald Melki^d and Andreas Heuer^{a,*}

^a*Behavioural Neuroscience Laboratory, Department of Experimental Medical Sciences, Lund University, Lund, Sweden*

^b*Department of Translational Neuroscience, Barrow Neurological Institute, Phoenix, AZ, USA*

^c*Molecular Neuromodulation, Department of Experimental Medical Sciences, Lund University, Lund, Sweden*

^d*Institut Francois Jacob (MIRCen), CEA and Laboratory of Neurodegenerative Diseases, CNRS, Paris, France*

^e*Basal Ganglia Pathophysiology, Lund University, Lund, Sweden*

Accepted 4 February 2022

Pre-press 23 February 2022

Abstract.

Background: Preclinical rodent models for Parkinson's disease (PD) based on viral human alpha-synuclein (h- α Syn) overexpression recapitulate some of the pathological hallmarks as it presents in humans, such as progressive cell loss and additional synucleinopathy in cortical and subcortical structures. Recent studies have combined viral vector-based overexpression of human wild-type α Syn with the sequential or simultaneous inoculation of preformed fibrils (PFFs) derived from human α Syn.

Objective: The goal of the study was to investigate whether sequential or combined delivery of the AAV vector and the PFFs are equipotent in inducing stable neurodegeneration and behavioral deficits.

Methods: Here we compare between four experimental paradigms (PFFs only, AAV-h- α Syn only, AAV-h- α Syn with simultaneous PFFs, and AAV-h- α Syn with sequential PFFs) and their respective GFP control groups.

Results: We observed reduction of TH expression and loss of neurons in the midbrain in all AAV (h- α Syn or GFP) injected groups, with or without additional PFFs inoculation. The overexpression of either h- α Syn or GFP alone induced motor deficits and dysfunctional dopamine release/reuptake in electrochemical recordings in the ipsilateral striatum. However, we observed a substantial formation of insoluble h- α Syn aggregates and inflammatory response only when h- α Syn and PFFs were combined. Moreover, the presence of h- α Syn induced higher axonal pathology compared to control groups.

*Correspondence to: Andreas Heuer, Behavioural Neuroscience Laboratory, Department of Experimental Medical Sciences, Lund University, Sölvegatan 19, 22 184 Lund, Sweden.; E-mail: andreas.heuer@med.lu.se.

Conclusion: Simultaneous AAV and PFF injections are equipotent in the presented experimental setup in inducing histopathological and behavioral changes. This model provides new and interesting possibilities for characterizing PD pathology in preclinical models and means to assess future therapeutic interventions.

Keywords: AAV, alpha synuclein, behavioral deficits, dopamine, inflammation, motor deficits, Parkinson's disease, phosphorylated synuclein, preclinical rodent model, preformed fibrils

INTRODUCTION

The most common preclinical rodent models of Parkinson's disease (PD) are produced by either injecting neurotoxicants, overexpressing PD-related genes, or by introducing mutations. Neurotoxicants such as 6-hydroxydopamine (6-OHDA) and 1-methyl-4-phenyl-1, 2, 3, 6-tetrahydropyridine (MPTP) cause a robust and rapid degeneration of the dopaminergic midbrain system, with subsequent behavioral impairments [1–6]. These approaches, however, neither replicate the alpha synuclein (α Syn)-linked pathology seen in PD patients [7, 8] nor the progressive neurodegeneration [9]. By contrast, genetic-based models, either transgenic animal lines or viral vector overexpression models, exhibit α Syn pathology although with variable levels of neurodegeneration and behavioral phenotypes. Viral vector-based overexpression of h- α Syn is a promising method to trigger the desired PD-like key features. The field has gone through several generations of viral vectors [10–13] and the most commonly used are recombinant adeno-associated viral (AAV) vectors. However, there is a great heterogeneity in the results from AAV-based studies in terms of α Syn expression levels, neurodegeneration, and behavioral deficits. This may be due to differences in expression systems and transgene cassettes such as promoter-transgene combinations, and posttranscriptional modifying and regulatory sequences (e.g., polyA and WPRE) as well as in the choice of capsid serotype, and in the quality control of the virus itself, resulting in variable success rate [11, 14–22]. Overexpression of clinical mutations such as the A53T variant [23–25], S129D and S129A [16, 26], and A30P [24] are an alternative to exacerbate relevant pathology. Moreover, increasing dosing of AAV to elicit a greater effect may confound the experimentation as the use of control vectors (e.g., GFP) can also confer a negative effect on the integrity of nigrostriatal neurons [27–30]. Nonetheless, in a typical experimental design, neurodegeneration seen in most AAV-based expression systems has been rather moderate with usually few

animals per experimental group displaying a stable behavioral phenotype.

The development of a reliable model is imperative in order to investigate the mechanisms of disease pathology as well as to test therapeutic interventions. High predictive and face-validity are needed to be able to translate approaches into clinical trials. As an example, glial cell line-derived neurotrophic factor (GDNF) showed great promise in the 6-OHDA model but failed to meet its primary endpoint in double-blind placebo-controlled clinical trials [31–35]. A direct comparison of the effects of GDNF between the 6-OHDA model and the α Syn model demonstrated neuroprotection only in the 6-OHDA model [36]. The availability of a robust model that mimics the progressive cell loss, α Syn pathology, and stable behavioral deficits is thus currently not widely available. In the attempt of accomplishing this aim, a more recent approach combines AAV vector-based overexpression methods with injection of pre-formed fibrils (PFFs), which seed endogenous α Syn inclusions [37–41]. PFFs have been injected either 4 weeks after an AAV- α Syn injection [37] or simultaneously [40, 42], with the latter approach being more practical and less invasive, requiring only a single surgical intervention. Finally, the combination of ectopic human α Syn together with PFFs derived from the human protein allows for studies focused on studying the human synucleinopathy with minimal interference from endogenous rodent α Syn. In the present study we directly compare the effects of the combination of human PFFs inoculation and AAV-h- α Syn in the midbrain of rats, either individually, combined, or after a 4-week delay. Pathological changes were assessed by immunohistochemical analysis, electrochemical recordings, and behavioral testing. The aims of the present study were i) to establish a model that generates stable behavioral phenotypes in the majority of animals, and ii) to investigate whether there is a difference in outcomes between the sequential or simultaneous PFFs injection approach.

We report that transgene expression along the nigrostriatal pathway in all the AAV-injected groups

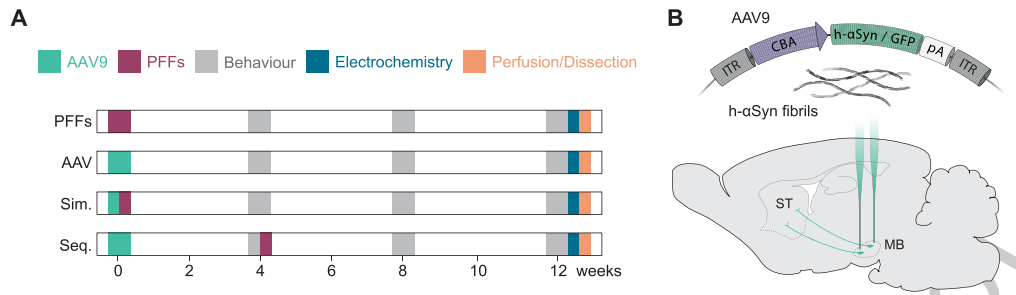


Fig. 1. Experimental layout. A) Description of the experimental groups and timepoints for behavioral test, electrochemical analysis, perfusions, and dissections. One group was injected with PFFs only (PFFs), two groups received either AAV-h- α Syn or AAV-GFP (AAV), two groups received AAV-h- α Syn or AAV-GFP and PFFs simultaneously (Sim.), and two groups received AAV-h- α Syn or AAV-GFP and PFFs sequentially (Seq.). B) Schematic of the pre-formed fibrils and viral genome expressing h- α Syn or GFP under the CBA promoter injected into the midbrain of rats. ITR, inverted terminal repeat; CBA, chicken β -actin; pA, polyadenylation site; h- α Syn, human alpha-synuclein; GFP, green fluorescent protein; PFFs, preformed fibrils; MB, midbrain; ST, striatum.

Table 1
Experimental groups. Schematic of the experimental groups and sample size for the analyses. Echem, electrochemistry; IHC, immunohistochemistry

| Group Name | Description | AAV injection | PFFs injection | N Tot | Behavior | FRET | Echem | IHC |
|----------------------|--------------|---------------|----------------|-------|----------|------|-------|-----|
| PFFs | PFFs only | – | week 0 | 8 | 8 | 3 | 3 | 5 |
| h- α Syn | AAV only | week 0 | – | 8 | 8 | 3 | 3 | 5 |
| h- α Syn/PFFs | Simultaneous | week 0 | week 0 | 10 | 10 | 3 | 3 | 7 |
| h- α Syn+PFFs | Sequential | week 0 | week 4 | 9 | 9 | 3 | 3 | 6 |
| GFP | AAV only | week 0 | – | 8 | 8 | 3 | 3 | 5 |
| GFP/PFFs | Simultaneous | week 0 | week 0 | 10 | 10 | 3 | 3 | 7 |
| GFP+PFFs | Sequential | week 0 | week 4 | 10 | 10 | 3 | 3 | 7 |

118 (both AAV-h- α Syn and AAV-GFP) produces down-
 119 regulation of tyrosine hydroxylase (TH) expression
 120 in the midbrain and striatum, irrespective of whether
 121 the AAV-vector was injected alone or in combina-
 122 tion with PFFs. These animals also displayed altered
 123 dopamine release and reuptake kinetics in electro-
 124 chemical recordings as well as motor impairments
 125 which did not recover over time. However, only when
 126 AAV-h- α Syn was combined with PFFs we observed
 127 phosphorylated α Syn similar to that seen in patient
 128 brains. Moreover, the combination of PFFs and
 129 AAV-h- α Syn triggered an enhanced inflammatory
 130 response around the area of transduction, which was
 131 not observed in the remaining experimental groups.
 132 Lastly, the presence of ectopic h- α Syn induced strong
 133 axonal pathology, with elevated numbers of striatal
 134 axonal swellings on the side of injection.

135 MATERIALS AND METHODS

136 Animals

137 All experimental procedures performed in this
 138 study were approved by the Malmö/Lund Ethics
 139 Committee on Animal Testing as well as according

to Swedish national guidelines (Jordbruksverket) 140
 and the EU Directive 2010/63/EU for animal 141
 experiments. Sixty-four adult (220–250 g) female 142
 Sprague-Dawley rats were purchased from Janvier 143
 Labs (France) and were housed under a 12:12 h 144
 dark:light cycle with *ad libitum* access to food and 145
 water in a temperature-controlled room in standard 146
 laboratory cages. A total of 64 rats were used in the 147
 current study and allocated randomly to the seven 148
 experimental groups. 149

150 Experimental outline

Naïve Sprague-Dawley rats (n=63) were ran- 151
 domly assigned into seven experimental groups 152
 receiving PFFs and AAV-vector overexpressing h- 153
 α Syn or GFP either alone or in combination (see 154
 Fig. 1 and Table 1). In the combination groups, one 155
 group received both PFFs and AAV simultaneously 156
 (h- α Syn/PFFs and GFP/PFFs) and in the other group 157
 PFFs inoculation followed the AAV injection sequen- 158
 tially after a four-week delay (h- α Syn + PFFs and 159
 GFP + PFFs). All rodents were subjected to a battery 160
 of behavioral tests at four-weeks intervals (i.e., week 161
 4, 8, and 12 after the first injection). Twelve weeks 162

163 after the first surgical session we performed electro-
164 chemical recordings for dopamine (DA) from three
165 anaesthetized rats per group. After all data was col-
166 lected, we either perfused the animals with PFA and
167 harvested the brains for immunohistochemistry (5–7
168 rats per group) or we harvested the brains (three rats
169 per group) for dissections of midbrain and striatum,
170 and snap-froze the tissue for subsequent quantifica-
171 tion of phosphorylated α Syn protein. A single rat was
172 injected with the neurotoxin 6-OHDA for histological
173 comparison.

174 *Preformed fibrils production*

175 Human wild type α Syn was expressed in *E. coli*
176 BL21 DE3 CodonPlus cells (Stratagene, San Diego,
177 CA, USA) and purified and assembled into the fib-
178 rillar polymorph “Fibrils” as described previously
179 [43]. Briefly, the protein (100 μ M) was incubated
180 in 50 mM Tris–HCl, pH 7.5, 150 mM KCl at 37°C
181 under continuous shaking in an Eppendorf Ther-
182 momixer set at 600 rpm for 5 days while withdrawing
183 aliquots (20 μ l) at different time intervals, mixing
184 them to Thioflavin T (10 μ M final) and recording
185 the fluorescence increase on a Cary Eclipse Fluores-
186 cence Spectrophotometer (Varian Medical Systems
187 Inc., Palo Alto, CA, USA) using an excitation wave-
188 length = 440 nm, an emission wavelength = 480 nm
189 and excitation and emission slits set at 2 and 5 nm,
190 respectively. The assembly reaction completion was
191 also assessed by sedimentation at 100,000 g at 25°C
192 for 30 min and measurement of the amount of pro-
193 tein remaining in the supernatant. The fibrillar nature
194 of α Syn was assessed by transmission electron
195 microscopy (TEM) after adsorption of the fibrils onto
196 carbon-coated 200 mesh grids and negative staining
197 with 1% uranyl acetate using a Jeol 1400 transmission
198 electron microscope. The images were recorded with
199 a Gatan Orius CCD camera (Gatan, Pleasanton, CA,
200 USA). The resulting α Syn fibrils were fragmented
201 by sonication for 20 min in 2 ml Eppendorf tubes in
202 a Vial Tweeter powered by an ultrasonic processor
203 UIS250v (250 W, 2.4 kHz; Hielscher Ultrasonic, Tel-
204 tow, Germany) to generate fibrillar particles with an
205 average size 42–52 nm as assessed by TEM analy-
206 sis. The final fibrils concentration was quantified to
207 be 350 μ M e.g., 5 μ g/ μ L. Fibrils were flash frozen
208 in liquid nitrogen (6 μ l aliquots) and stored at –80°C
209 until use. To defrost the samples, tubes were placed
210 in a water bath at 37°C and incubated for 3 min. After
211 incubation, samples were stored at room temperature
and utilized within the same day.

AAV production

212
213 AAV was produced as previously described
214 [44]. HEK293T cells were triple transfected with
215 either CBA-human α Syn or CBA-GFP, pAAV2/
216 9 and the helper plasmid pXX6. AAVs were purified
217 by iodixanol ultracentrifugation gradient and
218 concentrated using centrifugation columns (Orbital
219 Biosciences). Titration was performed using digi-
220 tal droplet PCR (ddPCR) with primers specific for
221 the ITRs (forward primer 5'-CGGCCTCAGTGAGC
222 GA-3' and reverse primer 5'-GGAACCCCTAGTG
223 ATGGAGTT-3'). The AAVs batches were diluted to
224 a working titer of 6×10^{12} gc/mL using modified PBS.

Stereotaxic surgery

225
226 Intracerebral injections were performed under
227 general anesthesia using Isoflurane (Attane vet
228 1000 mg/g, VM Pharma AB) in a 2% air mixture.
229 All working solutions containing viral vector and/or
230 PFFs were prepared so that the final concentrations
231 of viral vector and PFFs were 6×10^{12} gc/mL and
232 2.5 μ g/ μ L, respectively. Animals were head-fixed in
233 a stereotaxic frame with the incisor bar adjusted to
234 the flathead position (–4.5 mm below the interaural
235 line). Each solution was infused unilaterally into the
236 midbrain using a pulled glass capillary attached to a
237 10 μ L Hamilton syringe. The following coordinates
238 (from Bregma, in mm) and volumes were utilized:
239 2 μ L at AP = –5.3, ML = –0.8, DV = –7.5 and 2 μ L
240 at AP = –5.6, ML = –2.3, DV = –7.5 with an infusion
241 rate of 0.5 μ L/min. After injection, the syringe was
242 left in place for additional 3 min and thereafter slowly
243 retracted. 6-OHDA was injected as described previ-
244 ously [45]. In brief, 5.41 μ g/ μ L 6-OHDA (calculated
245 from free-base 6-OHDA-HBr salt, Sigma) was dis-
246 solved in 0.2 mg/ml ascorbic acid in 0.9% sterile
247 saline and a volume of 3 μ L was injected at the fol-
248 lowing coordinates AP = –4.0, ML = –1.3, DV = –7.0.
249 The injection speed was set to 1 μ L/min and the nee-
250 dle was left in place for an additional 3 min to allow
251 for diffusion of the toxin.

Behavioral analysis

252
253 All behavioral assessment was performed at 4, 8,
254 and 12 weeks after lesion by the same researcher,
255 blind to the rats' treatment group.

Drug-induced rotations

256
257 Rats were injected i.p. with 2.5 mg/kg *d*-ampheta-
258 mine (Apotheksbolaget) and placed in automated

259 rotameter bowels modelled after the design of Unger-
260 stedt [6, 46]. All full ipsilateral and contralateral
261 rotations, with respect to the side of injection, were
262 quantified over 90 min. The data are presented as
263 average rotations per minute.

264 *Stepping test*

265 Forelimb akinesia was assessed by quantifying
266 forelimb adjusting steps as previously described [47,
267 48]. In brief, rats were constrained by the experi-
268 menter so that only one forelimb was freely movable.
269 The animal was moved sideways over 90 cm at a
270 constant speed. The number of both backward and
271 forward adjusting steps was counted three consec-
272 utive times for each paw. Out of the three trials, the
273 best two trials, in terms of number of steps performed,
274 were averaged, and adjusting steps data was presented
275 as percentage bias.

276 *Cylinder test*

277 Forelimb asymmetry in exploratory behavior was
278 assessed by placing the animals in a glass cylin-
279 der and recording with a digital video camera for
280 a total of 5 min [49]. The number of right and left
281 forepaw weightbearing touches for a total of 20
282 touches was counted *post-hoc* by a blinded researcher
283 and the score was expressed as percentage bias. Two
284 GFP/PFFs rats were removed from the final analysis
285 of the Cylinder test at week 4, two h- α Syn rats, three
286 GFP rats, one GFP/PFFs rat and one GFP + PFFs rat
287 at week 8, three GFP rats, two GFP/PFFs rats and
288 two GFP + PFFs rats at week 12 due to a failure to
289 complete at least 15 touches.

290 *Electrochemistry*

291 *In vivo* electrochemical chronoamperometric
292 recordings were performed as previously described
293 [50, 51] using Nafion®-coated carbon fiber elec-
294 trodes (\emptyset 30 μ m, L 150 μ m, Quanteon) coupled
295 to FAST-16mkII hardware (Quanteon). DA release
296 was induced by local injection of 220–240 nL
297 KCl (120 mM, pH = 7.4) through a glass capillary
298 connected to a picospritzer (Aldax) micropressure
299 system (15–20 PSI for 0.1–0.5 s). The glass capillary
300 was mounted \sim 50–100 μ m from the electrode tip.
301 Before the recording, each electrode was calibrated
302 in 0.1 M PBS. Only electrodes with a linear response
303 rate to three 2 μ M additions of DA ($r^2 < 0.995$) were
304 selected. Moreover, only electrodes that displayed a
305 selectivity of 1:100 over ascorbic acid and a limit of
306 detection smaller than 0.01 mM DA were used [52].

307 During *in vivo* recordings, an Ag/AgCl reference
308 electrode was used which was previously prepared
309 by electroplating an Ag wire in NaCl-saturated 1 M
310 HCl solution. High-speed (4 Hz) chronoamperomet-
311 ric recordings were performed by applying a square
312 wave potential (+0.55 V; 0 V resting) and the result-
313 ing oxidation and reduction currents were analyzed
314 using the F.A.S.T. analysis software. For each record-
315 ing, the electrode-micropipette assembly was left in
316 the recording site for at least 30 min to stabilize before
317 4 recordings were made at 10 min intervals.

318 *Perfusion*

319 Animals were given a terminal anesthetic dose
320 of Sodium Pentobarbital i.p. and transcardially per-
321 fused by infusing approximately 150 mL of 0.9%
322 saline solution at RT, followed by 250 mL ice-cold
323 4% paraformaldehyde (PFA, pH = 7.4) in 0.1 M phos-
324 phate buffer. After perfusion, the brain was removed
325 from the skull and stored in 4% PFA solution for
326 additional 24 h before being transferred into a 25%
327 sucrose and 0.01% Na₃N solution where they were
328 kept until they sunk.

329 *Immunohistochemistry*

330 Brains were sectioned on a freezing sledge micro-
331 tome (Leica) at a section thickness of 40 μ m and
332 collected in a 1:12 series. Sections were stored
333 in antifreeze solution at -20°C until further use.
334 The protocol for immunohistochemistry has been
335 described elsewhere [53] and a list of the primary and
336 secondary antibodies used can be found in Table 1.
337 Briefly, tissue sections were washed (3x) in potassium
338 phosphate buffered saline (KPBS, pH = 7.4) and then
339 incubated for 15 min in 3% H₂O₂, 10% methanol in
340 PBS to quench endogenous peroxidase activity. After
341 (3x) PBS washes, sections were incubated for 1 h in
342 blocking solution consisting of 5% serum in KPBS
343 and 0.25% Triton X-100 (TPBS, pH = 7.4). The sec-
344 tions were then incubated in primary antibody in 5%
345 serum overnight at room temperature. On the second
346 day, sections were rinsed with (2x) KPBS and subse-
347 quently incubated in 5% serum for 1 h before being
348 incubated for 1 h in secondary antibody solution in
349 5% serum. The secondary antibody was removed
350 by (3x) KPBS washes and sections were incubated
351 in avidin-biotin-peroxidase complex (ABC, Vector-
352 labs) in KPBS for 1 h. After an additional (3x) KPBS
353 washes sections were incubated for 2–10 min in a
354 peroxidase (HRP) detection system (Vector® DAB,

Table 2
Antibodies and dyes used in the current study for immunohistochemical analysis

| Antibody | Species | Cat. no | Concentration |
|---------------------------------|---------|----------|---------------|
| Human α Synuclein 211 | Mouse | SC-12767 | 1:1000 |
| GFP | Chicken | A10262 | 1:10000 |
| α Synuclein, p-S129 | Rabbit | ab51253 | 1:100000 |
| α Synuclein 81A (p-S129) | Mouse | AB184674 | 1:10000 |
| CD11b (Ox42) | Mouse | MCA275G | 1:500 |
| TH | Sheep | ab113 | 1:750–1:1000 |
| TH | Mouse | MAB318 | 1:1000 |
| VMAT2 | Rabbit | 20042 | 1:10000 |
| Ubiquitin | Rabbit | AB7780 | 1:200 |
| ThioflavinS | - | T1892 | 1:100 |
| DAPI | - | D9542 | 1:2000 |
| Anti-rabbit Biotinylated | Goat | BA6000 | 1:200 |
| Anti-mouse Biotinylated | Horse | BA2001 | 1:200 |
| Anti-chicken Biotinylated | Goat | BA9010 | 1:200 |
| Anti-sheep Alexa 488 | Donkey | A11015 | 1:500 |
| Anti-chicken Alexa 488 | Chicken | A11039 | 1:500 |
| Anti-rabbit Alexa 488 | Goat | A11008 | 1:500 |
| Anti-rabbit Alexa 568 | Goat | A11011 | 1:500 |
| Anti-mouse Alexa 568 | Goat | A11004 | 1:500 |
| Anti-mouse Alexa 647 | Donkey | A31571 | 1:500 |
| Anti-rabbit Alexa 647 | Goat | A21245 | 1:500 |

Vector Laboratories). The sections were mounted on gelatine-coated glass slides, dehydrated in an ascending series of ethanol (70%, 95%, 99.5%, 99.5%) for 2 min each, followed by (2x) 2 min incubations in xylene to remove lipids and cover-slipped using DPX mounting medium. For fluorescence immunohistochemistry, the quenching step, the ABC incubation, and the DAB reaction were skipped; instead, sections were incubated for 1 h in fluorophore-conjugated secondary antibody, washed (3x) in KPBS, mounted onto gelatine-coated glass slides and cover-slipped as soon as dry using PVA/DABCO solution. When DAPI was needed, sections were incubated for 5 min at RT before the last washing step. Thioflavin S coloration was executed as describes elsewhere [54].

Proteinase K treatment

Coronal sections were mounted on permafrost-glass slides and were incubated in proteinase K solution (25 μ g/mL; QIAGEN) for one hour at room temperature before proceeding with the immunostaining for pSer129 as described above.

Dissections

Three rats per group were sacrificed by decapitation at 13 weeks post-injection. Brains were extracted, rinsed in 0.9% saline solution, and coronally sectioned using a rat brain matrix on ice. The

striatum and midbrain from each hemisphere were dissected using sterile razor blades. Tissue samples were snap-frozen in isopentane on dry ice and stored in 1.5 mL Eppendorf tubes at -80°C until further processing.

Brain tissue homogenization

Frozen tissues were weighed in 2 ml Eppendorf tubes. The samples were diluted ten times in 150 mM KCl, 50 mM Tris-HCl pH 7.5 to obtain a homogenate at 10% (weight:volume). The homogenization was performed by sonication using the SFX 150 Cell Disruptor sonicator with a 3.17 mm microtip probe (Branson) for 15 s, with 1 s pulses followed by 1 s pauses in a biosafety level 3 environment (BSL-3). The homogenates were aliquoted and immediately frozen in liquid nitrogen before storage at -80°C . All contaminated surfaces were cleaned with SDS (1%) [55].

Protein quantification

The quantification by TR-FRET of phosphorylated α Syn at Ser-129 or aggregated α Syn was performed using a fluorescence resonance energy transfer (FRET) assay (Cisbio, France, cat #6FSYN-PEG and # 6FASYPEG respectively). Briefly, the brain homogenates were diluted to 5% (W:V) in lysis buffer provided in the HTRF kit. For phosphorylated α Syn assay, 16 μ L of each diluted brain homogenates were loaded into a 96 well plate and mixed with 4 μ L of the FRET donor and acceptor antibodies in the kit. For aggregated α Syn assay, 10 μ L of each diluted brain homogenates were loaded into a 96 well plate and mixed with 10 μ L of the FRET donor and acceptor antibodies in the kit. The plates were sealed with a film (CmlAB, Denmark, cat #13076-9P-500) and incubated for 20 h at 20°C without shaking in a Thermomixer comfort (Eppendorf, Montesson, France). Time-resolved FRET was measured after incubation upon excitation at 337 nm using a plate reader (CLARIOstar, BMG Labtech, Germany) as described [56]. The HTRF signal was recorded at two different wavelengths (665 nm and 620 nm). The amount of aggregated α Syn was derived from the 665/620 nm fluorescence ratio and multiplied by 10000.

Densitometry

High resolution scans were taken with an Epson flatbed scanner at 600 DPI. The level of staining

intensity was measured from 4 striatal sections (AP + 1.6, + 0.7, -0.26, and -0.6 mm) for α Syn211-DAB, GFP-DAB and TH-DAB and one midbrain section (AP: -5.6 mm) for OX42-DAB, using ImageJ software (NIH, Version 1.8.0). Before measurement, each image was transformed into grayscale 8-bit and calibrated using a step-tablet from Epson with known OD values using the Rodbard function (<https://imagej.nih.gov/ij/docs/examples/calibration/>). Correction for non-specific background was done by subtracting values obtained from the corpus callosum to the measured values. The regions of interest were outlined, and the grey-pixel intensity value average was measured. The data are expressed as optical density values of contralateral vs ipsilateral striatum or midbrain.

Stereology

Quantification of TH⁺ cells in the SNpc was performed according to the optical fractionator principle using ImageJ Software (NIH, Version 1.8.0) [57]. In brief, z-stack images of every sixth series (section sampling fraction, $ssf = 1/6$) of the SNpc region were acquired at 20X magnification using a Leica DMi8 microscope, which yielded to 8–10 sections per animal. The average mounted section thickness (t) was $20 \pm 2.6 \mu\text{m}$ and the height of optical dissector (h) used was $12 \mu\text{m}$ ($3 \mu\text{m}$ guard zones). Grid area was set at $170 \times 170 \mu\text{m}^2$ and the counting frame size at $55 \times 55 \mu\text{m}^2$. A maximal coefficient of error (CE) of 0.11 for the intact side was accepted and animals with higher CE values were excluded from the analysis.

Axonal swellings quantification

Quantification of striatal axonal swellings was performed following α Syn211, GFP and TH DAB-IHC. Three high-resolution 63X z-stacks were taken from central, dorso-medial, and dorso-lateral regions of the striatum as previously described [19]. Each z-stack had a z-step size of $1 \mu\text{m}$ for a total of 30 z-steps. The ImageJ 3D object count tool was used to identify the swellings and calculate their total number, as well as their volume, by setting an exclusion threshold for particles $< 4 \mu\text{m}^3$ and circularity between 0.5–1.0. The average number and volume size of swellings was calculated based on the total swelling number from all the three pictures from one animal and for Fig. 7M and 7O and Supplementary Figure 5G and 5I were divided in small ($4\text{--}10 \mu\text{m}^3$), medium ($10\text{--}20 \mu\text{m}^3$) and large ($> 20 \mu\text{m}^3$).

Statistics

All data were analyzed using the statistical software GraphPad Prism (V 8.4.3) using an alpha of 0.05 as threshold for determining statistical significance. For group and group by side analysis we performed analysis of variance with the factors Group and Side as dependent variables. For time-course analysis we performed repeated measures ANOVAs with the factors Week and Group. *Post hoc* testing used Sidak's correction were applied to avoid Type 1 errors/inflating alpha due to multiple comparison testing.

RESULTS

In the current study we injected PFFs and/or α Syn overexpressing AAV either individually or in combination, simultaneous or sequentially after a 4-week delay, to induce a pathologically relevant level of neuronal cell loss in the midbrain of rats.

Injection of AAV-h- α Syn leads to strong overexpression of α Syn along the nigrostriatal pathway

We first assessed the expression of h- α Syn throughout the nigrostriatal pathway at 12 weeks following vector delivery. The groups injected with AAV-h- α Syn displayed strong α Syn immunoreactivity on the injected side of the midbrain with evident spread along dopaminergic nigrostriatal projections (Fig. 2A-D) with some diffusion into the contralateral hemisphere in the midbrain. The comparison of the staining intensity between the left and right striatum (Fig. 2E) for the four treatment groups showed that there was a significant difference in human synuclein immunoreactivity between the groups and the side of the brain analyzed (Groups*Side, $F_{3,18} = 6.88$, $p < 0.01$). All groups injected with AAV-h- α Syn displayed a similar degree of α Syn immunoreactivity which was absent in the group that received PFFs only (*Sidak*, all $p < 0.0001$). Triple immunofluorescent immunoreactivity for the enzyme tyrosine-hydroxylase (TH), the Vesicular Monoamine Transporter 2 (VMAT2), and α Syn211 (human α Syn) confirmed that the midbrain dopaminergic neurons of the PFFs-inoculated group did not express h- α Syn (Fig. 2F-F_{iii}), whereas all groups receiving the AAV-vector expressed h- α Syn throughout most of the midbrain dopamine neurons (Fig. 2G-I_{iii}). The lack of staining in the PFFs treated

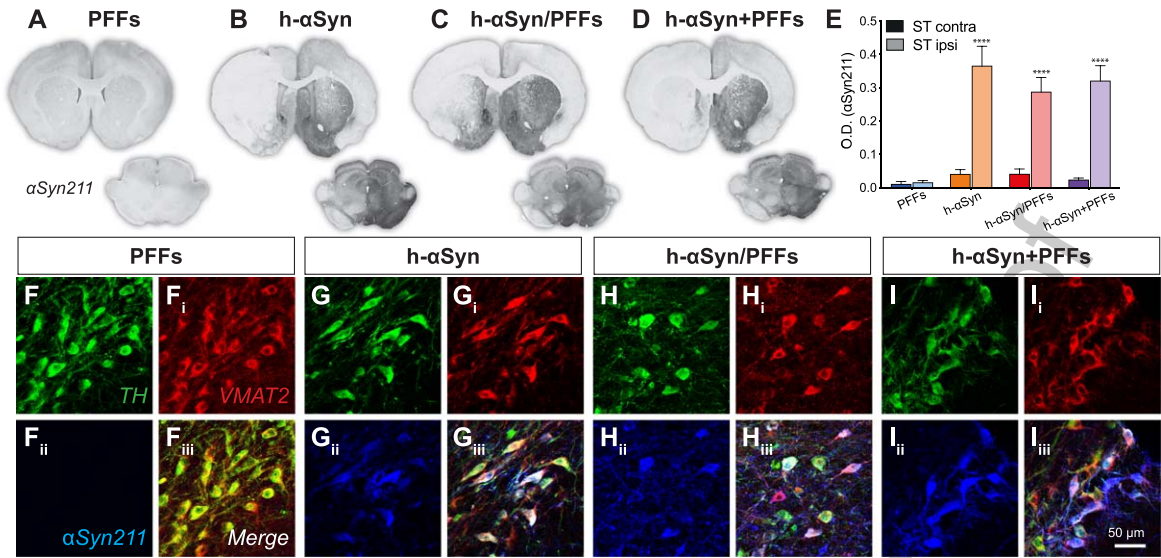


Fig. 2. AAV-vector overexpression. A-D) Representative midbrain and striatal sections for each group stained for human α Syn (α Syn211). E) Densitometric analysis comparing human α Syn211 staining intensity between contralateral and ipsilateral right striatum. F-I_{iii}) Triple immunofluorescence demonstrating colocalization between TH, VMAT2, and α Syn211 antibodies in SNpc. PFFs, preformed fibrils; h- α Syn, human alpha-synuclein; contra, contralateral; ipsi, ipsilateral; O.D., optical density. Data are expressed as mean \pm SEM. (**** $p < 0.0001$).

521 group is not surprising as the 211 antibody is directed
 522 against the C-terminal end of the human protein,
 523 which is known to be cleaved off rapidly [58]. Similar
 524 results were observed for the GFP expression in the
 525 control groups (Supplementary Figure 1A-C) where
 526 we observed a significant difference in GFP expres-
 527 sion between left and right side (Side, $F_{1,13} = 67.40$,
 528 $p < 0.0001$). Indeed, all groups that were injected
 529 with AAV-GFP displayed a similar degree of GFP
 530 immunoreactivity in the ipsilateral side compared
 531 to the contralateral side (Supplementary Figure 1D,
 532 *Sidak*, all $p < 0.01$). Triple immunofluorescence for
 533 TH, VMAT2 and GFP further confirmed that all the
 534 AAV-GFP injected groups were expressing GFP in
 535 midbrain dopaminergic neurons (Supplementary Fig-
 536 ure 1E-G_{iii}).

537 *Strong transgene overexpression results in TH* 538 *downregulation in the striatum and midbrain*

539 After confirming AAV-mediated expression levels,
 540 we investigated whether overexpression of h- α Syn
 541 was sufficient to induce a change in the nigrostriatal
 542 DA system. We performed immunohistochemical
 543 labelling on serial sections for the rate-limiting
 544 enzyme in dopamine production, TH, as a proxy
 545 marker for dopaminergic neurons (Fig. 3A-D) and
 546 demonstrate that in rats injected with the AAV-vector
 547 alone or in combination, but not with PFFs alone,

548 there was an overt reduction in TH immunoreac-
 549 tivity in the striatum and midbrain ipsilateral to the
 550 injection. Optical density measurements in the stri-
 551 atum confirmed that there was a difference in TH
 552 staining intensity between groups and hemisphere
 553 (Fig. 3H, Group*Side, $F_{3,17} = 12.04$, $p < 0.001$). All
 554 three AAV-h- α Syn injected groups, but not the PFFs
 555 group, displayed a reduction in ipsilateral TH stain-
 556 ing intensity which was on average by $52.86\% \pm$
 557 5.12 (Fig. 3H, *Sidak*, all $p < 0.0001$). Surprisingly,
 558 we observed similar results when GFP was overex-
 559 pressed (Fig. 3E-G). Densitometric analysis of the
 560 AAV-GFP injected animals revealed a significant
 561 reduction by $69.01\% \pm 9.00$ in TH staining inten-
 562 sity in the ipsilateral side (Fig. 3I, Side $F_{1,13} = 54.10$,
 563 $p < 0.0001$, *Sidak*, all $p < 0.01$).

564 To quantify the degree of TH+neuron loss in
 565 the midbrain we performed unbiased stereological
 566 counting of TH immunoreactive cells in the mid-
 567 brain in the ipsi- and contralateral SN (Fig. 3J).
 568 There was a significant difference in the number
 569 of TH immunoreactive cells in the SNpc between
 570 the groups and the brain side (Fig. 3J; Group*Side,
 571 $F_{6,24} = 4.96$, $p < 0.01$). All AAV-h- α Syn injected
 572 groups, but not the PFFs group, displayed a difference
 573 between the absolute TH⁺-cell numbers counted
 574 between the injected and non-injected side (*Sidak*,
 575 all $p < 0.05$). In particular, the TH⁺ cell loss in PFFs,
 576 h- α Syn, h- α Syn/PFFs, and h- α Syn+PFFs groups was
 577

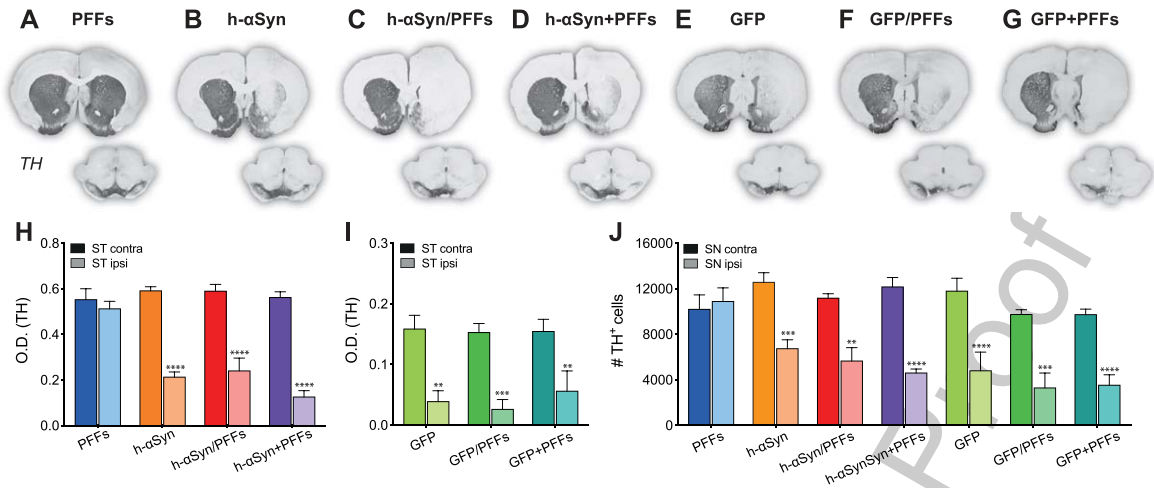


Fig. 3. TH downregulation in striatum and substantia nigra. A-G) TH immunoreactivity from representative midbrain and striatal sections. H-I) Densitometric analysis comparing TH staining intensity between left and right striatum. J) Cell count of TH⁺ cells in the SNpc represented as number of TH⁺ cells between contralateral and ipsilateral SNpc. PFFs, preformed fibrils; h- α Syn, human alpha-synuclein; GFP, green fluorescent protein; ST, striatum; SN, substantia nigra pars compacta; O.D., optical density. Data are expressed as mean \pm SEM. (** $p < 0.01$, *** $p < 0.001$, **** $p < 0.0001$).

577 $-3.29\% \pm 4.44$, $31.10\% \pm 3.29$, $34.57\% \pm 10.91$,
 578 and $44.68\% \pm 4.90$ respectively. Quantification for
 579 the AAV-GFP injected groups revealed a reduction
 580 in TH⁺ cells in the ipsilateral side similar to
 581 that observed for the AAV-h- α Syn injected groups
 582 (*Sidak*, all $p < 0.001$). Specifically, the TH⁺ cell
 583 loss in GFP, GFP/PFFs, and GFP+PFFs groups was
 584 $46.38\% \pm 15.72$, $52.80\% \pm 14.12$, and $50.23\% \pm 11.04$
 585 respectively. Although the TH⁺ loss in the three AAV-
 586 GFP groups seemed to be higher compared to the loss
 587 observed in the three AAV-h- α Syn groups, the compar-
 588 ison between counts in the ipsilateral side did not
 589 reach statistical significance (*Sidak*, all n.s.). Three h-
 590 α Syn/PFFs rats, one h- α Syn+PFFs rat, one GFP rat,
 591 three GFP/PFFs rats, and one GFP+PFFs rat were
 592 excluded from the stereological counting due to a
 593 coefficient of error (CE) bigger than 0.11.

594 Although TH is often used as a proxy marker
 595 for cell loss, it does not reveal whether the mid-
 596 brain dopamine neurons have degenerated or whether
 597 there was a mere downregulation of expression as a
 598 result of α Syn pathology [27]. To address this ques-
 599 tion, we performed immunohistochemistry for TH
 600 and NeuN, a pan-neuronal marker. We observed both
 601 a loss of TH and NeuN immunoreactive cells ipsi-
 602 lateral to the injection in all groups injected with
 603 the AAV-h- α Syn alone or in combination with PFFs,
 604 but not in the PFFs-only group (Supplementary Fig-
 605 ure 2A-D_{ii}). A comparison between the AAV-h- α Syn
 606 model and the 6-OHDA model showed that the loss

of NeuN immunoreactive cells is not restricted to the
 anatomical location of the SNpc (Supplementary Fig-
 ure 2E-E_{ii}). These observations suggest that the α Syn
 pathology caused a combination of TH downregula-
 tion and overt neurodegeneration.

Transgene overexpression results in behavioral impairments with or without additional insult with PFFs

Assessment of motor function was performed
 at 4, 8, and 12 weeks after the first surgery. To
 assess forelimb akinesia and asymmetry we per-
 formed stepping and cylinder tests, respectively.
 Unilateral depletion of dopaminergic signaling was
 assessed additionally through drug-induced rotation
 test after *d*-amphetamine injection and eventually
 through electrochemical detection of striatal DA
 release.

To facilitate the visualization of the seven groups in
 the behavioral analyses, graphs for h- α Syn (Fig. 4A,
 C, E) and GFP control (Fig. 4B, D, F) groups
 were kept separate; however, statistical analyses
 were performed with all groups together. Across the
 three post-injection timepoints, animals in the three
 AAV-h- α Syn injected groups and AAV-GFP injected
 groups displayed a bias to neglect the paw contralat-
 eral to the side of the lesion, whereas animals in
 the PFFs-alone group did not display a side bias
 (Fig. 4A, B). The deficit in the Cylinder test was

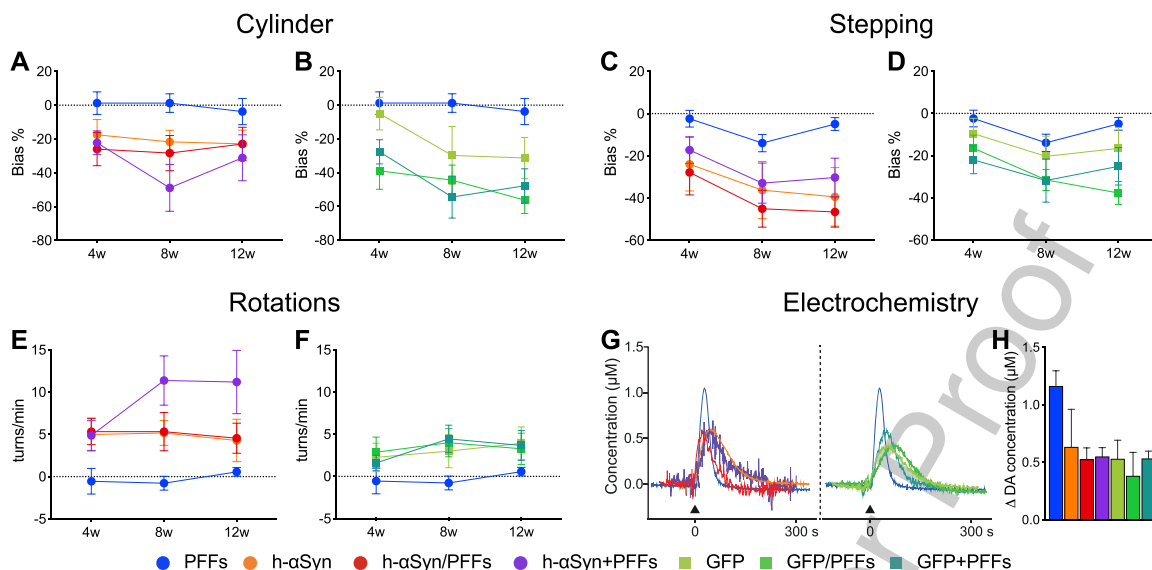


Fig. 4. Behavioral impairments following h- α Syn and/or PFFs injection. A-F) Behavioral tests performed to assess motor function at 4-, 8-, and 12-weeks post-injection for Cylinder, Stepping, and Rotation test for the h- α Syn (circles, A, C, E), GFP (squares, B, D, F), and PFF (circles, A-F) injected groups, respectively. G) Electrochemical recordings (chronoamperometry) for KCl-evoked striatal DA release; black arrow indicates the timepoint of KCl application. H) Average peak amplitude, reflecting the maximum amount of dopamine available, for all the seven experimental groups. PFFs, preformed fibrils; h- α Syn, human alpha-synuclein; GFP, green fluorescent protein; w, weeks; s, seconds. Data are expressed as mean \pm SEM. Note: the behavioral results of the PFFs group are duplicated in each graph for ease of comparison.

635 slightly more pronounced at week 8 and 12 post-
 636 injection (Week, $F_{2,96} = 6.54$, $p < 0.05$); however, this
 637 effect was not significantly different for the groups
 638 (Week*Group, $F_{12,96} = 1.33$, $p = ns$). Similar to the
 639 Cylinder test, animals in the AAV-h- α Syn and AAV-
 640 GFP injected groups performed fewer adjusting steps
 641 on the stepping test compared to their PFFs-only
 642 injected counterparts (Fig. 4C, D). Again, there was
 643 a significant effect of time (Week, $F_{2,112} = 11.08$,
 644 $p < 0.0001$) with performance in week 4 being sig-
 645 nificantly less pronounced than that in weeks 8 and
 646 12 (*Sidak*, $p < 0.001$), indicating a progressive phe-
 647 notypic evolution of the behavioral deficit on this
 648 test. The most commonly used test to assess a uni-
 649 lateral depletion of dopamine is the drug induced
 650 rotation test. Here we injected the rats with 2.5 mg/kg
 651 *d*-amphetamine and recorded the rotational behavior
 652 for 90 min. As can be seen in Fig. 4E and F, a strong
 653 net contralateral rotational response was seen already
 654 at the 4 weeks timepoint for all the AAV-h- α Syn
 655 injected groups, whereas the PFFs-alone injected
 656 group did not display any rotational behavior and the
 657 AAV-GFP injected groups had a lower rotational
 658 response. Indeed, there was a significant effect of
 659 week (Week, $F_{2,112} = 3.19$, $p < 0.05$). Over time, all
 660 groups maintained a stable behavioral phenotype,

except for the h- α Syn + PFFs group which increased
 its rotational response at 8 and 12 weeks.

One major challenge of the protein over-
 expression model is the difficulty to establish
 clear histopathological thresholds for predicting
 behavioral impairments. Whereas in the classical
 neurotoxicant-based models (e.g., 6-OHDA) a loss
 of 70–80% of dopaminergic neurons is necessary to
 induce behavioral deficits, in the AAV vector-based
 models cell loss is not necessary to see behavioral
 effects. In the toxicant-based models, cell loss is a
 rather binary event where the cells are either in the
 process of dying or already degenerated. However,
 an important aspect of the vector-based models is
 that neurons can be still alive, albeit severely dys-
 functional. To address the neuronal function, we
 performed electrochemical recordings to investigate
 the DA release and reuptake kinetics of the remain-
 ing dopaminergic fibers in the striatum. As can be
 seen from the representative traces of individual ani-
 mals (Fig. 4G) local KCl application resulted in a
 reduced peak amplitude in all the groups compared
 to the PFFs only group. Overall, the peak amplitude,
 which reflects the maximum amount of DA available,
 was lower in all the AAV-injected groups compared
 to the PFFs only group (Fig. 4H). These results are

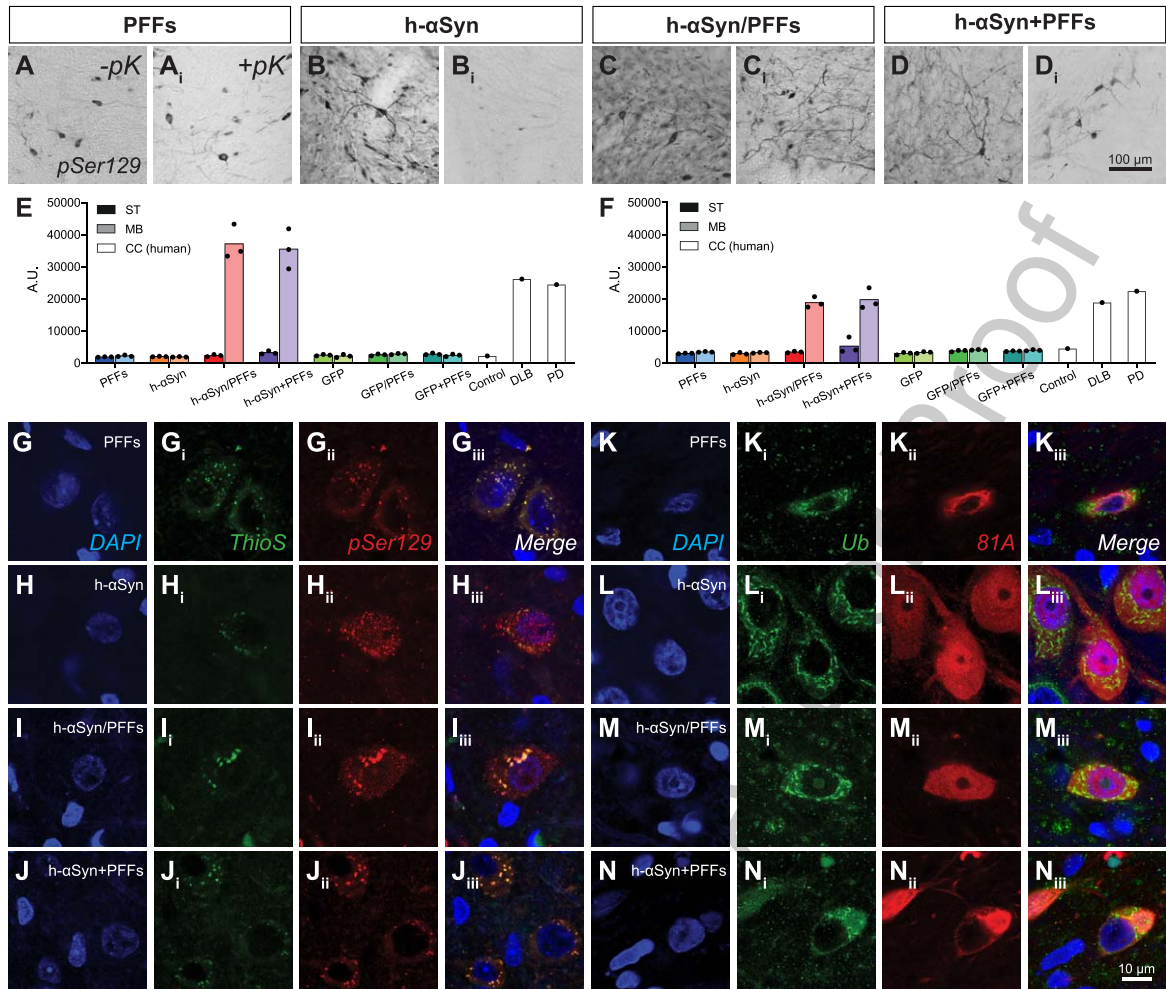


Fig. 5. h- α Syn overexpression and PFFs treatment results in Lewy-like midbrain pathology. A-D_i) pSer129 immunoreactivity in midbrain before (-pK) and after (+pK) proteinase K treatment. E, F) TR-FRET quantification of pSer129 (E) and aggregated α Syn (F) in the ipsilateral midbrain and striatum of rats and cingulate cortex of human samples. Black dots represent single subjects. G-J_{iii}) Triple immunofluorescence showing co-localization between pSer129 and Thioflavin S. K-N_{iii}) Triple immunofluorescence showing co-localization between 81A (pSer129) and Ubiquitin antibodies. PFFs, preformed fibrils; h- α Syn, human alpha-synuclein; pK, Proteinase K; Ub, ubiquitin; ThioS, Thioflavin S; ST, striatum; MB, midbrain; CC, cingulate cortex. (A.U. = ratio 665 nm/620 nm multiplied by 10000).

687 in line with the behavioral deficits and TH down-
 688 regulation and associated behavioral deficits reported
 689 above and suggest that surviving dopaminergic cells
 690 are dysfunctional.

691 *h- α Syn overexpression and PFFs inoculation*
 692 *results in parkinsonian-like pathology and*
 693 *inflammatory response*

694 In human PD, α Syn in Lewy bodies is sub-
 695 jected to post-translational modifications, such as
 696 phosphorylation and ubiquitination [59–61]. More-
 697 over, it is known that α Syn fibrils are forming
 698 when α Syn assembles in repeated β -sheet structures,

699 which can be recognized by amyloid-specific dyes
 700 such as Thioflavin S [62]. Accordingly, we investi-
 701 gated whether our samples displayed α Syn inclusions
 702 with similar histopathological features. pSer129
 703 immunoreactive cells can be detected in the surviving
 704 DA neurons in the ipsilateral side in all four target
 705 groups (Fig. 5A-D_i, Supplementary Figure 3A-D_{ii})
 706 but not in control groups (Supplementary Figure 3E-
 707 G_{ii}). Importantly, the phosphorylated α Syn inclu-
 708 sions found in all target groups receiving PFFs were
 709 resistant to proteinase K-digestion (pK), a feature that
 710 is a key characteristic of the Lewy body (Fig. 5A_i,
 711 C_i, D_i). Although there was a substantial amount of punc-
 712 tuate pSer129-immunoreactivity in the AAV-h- α Syn

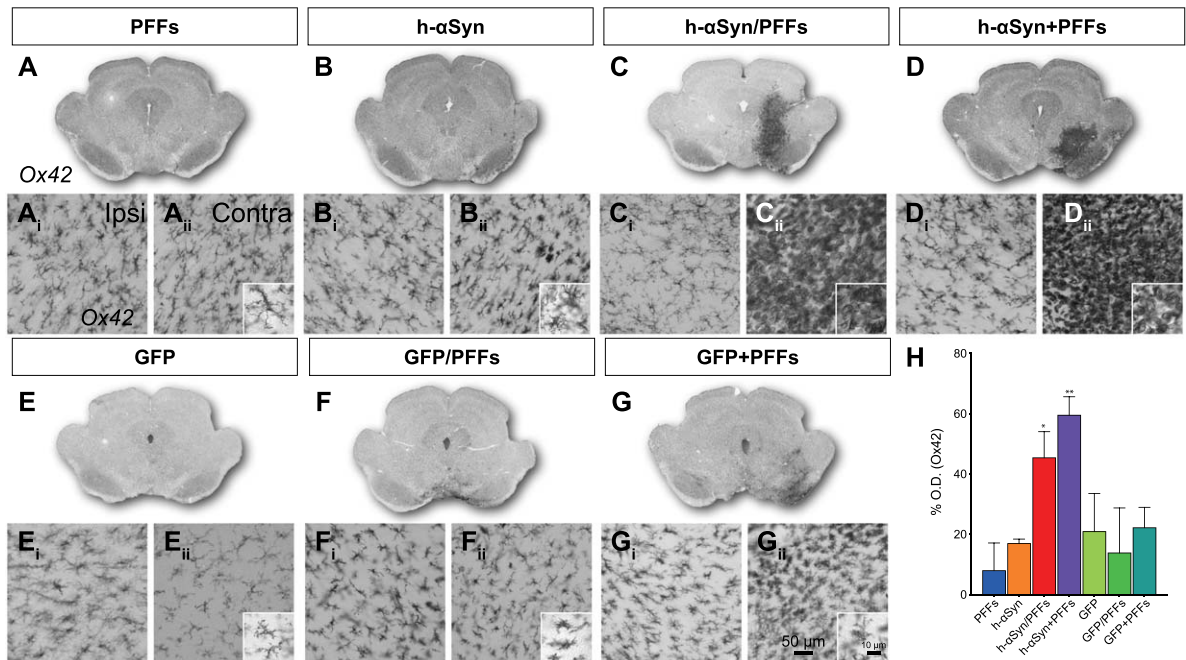


Fig. 6. Inflammatory response. A-G) Overviews of rat midbrain sections stained for Ox42. A_i-G_{ii}) Close-up 20X images for Ox42 immunoreactivity in contralateral (A_i-G_i) and ipsilateral (A_{ii}-G_{ii}) side for target and control groups and additional 63X magnification images (A_{ii}-G_{ii}) for the ipsilateral side. H) Densitometric analysis showing the increase in percentage for Ox42 staining intensity in the ipsilateral midbrain (vs. contralateral) for target and control groups. PFFs, preformed fibrils; h-αSyn, human alpha-synuclein; GFP, green fluorescent protein; Ipsi, ipsilateral; Contra, contralateral. Data are expressed as mean ± SEM. (* $p < 0.05$, ** $p < 0.01$).

713 group, after pK-digestion, only little immunoreactiv- 737
 714 ity remained (Fig. 5B_i). Quantitatively, h-αSyn/PFFs 738
 715 and h-αSyn + PFFs treated groups showed levels of 739
 716 phosphorylated αSyn (Fig. 5E) and aggregated αSyn 740
 717 (Fig. 5F) in the ipsilateral midbrain comparable to 741
 718 that seen in the brains of human patients with Lewy 742
 719 body dementia or PD. The remaining groups displayed 743
 720 no significant amount of phosphorylated αSyn neither 744
 721 in midbrain nor striatum (data not shown). 745
 722 The lack of p-αSyn or aggregated αSyn in the striatum 746
 723 is not surprising as the timeframe of this study 747
 724 (12 weeks) is likely insufficient for the spread and 748
 725 seeding of pathological αSyn to target areas [37, 63]. 749

726 Even though detectable levels of aggregated αSyn 750
 727 in midbrain were present only in h-αSyn/PFFs and 751
 728 h-αSyn+PFFs groups, all four target groups showed 752
 729 pSer129⁺ and ThioS⁺ inclusions (Fig. 5G-J_{iii}) and 753
 730 pSer/81A⁺ and Ub⁺ inclusions (Fig. 5K-N_{iii}), which 754
 731 resemble the histopathological hallmarks presented 755
 732 in human Lewy pathology. 756

733 It has been hypothesized that neurodegeneration 757
 734 in PD may result from inflammation in response to 758
 735 abnormal forms of αSyn [64, 65]. We therefore investi- 759
 736 gated whether our samples showed any alteration 760

737 in the inflammatory response and particularly in 738
 739 microglia activation (Fig. 6A-G). The combination 740
 741 of h-αSyn and PFFs led to a strong microglial activa- 742
 743 tion in the ipsilateral side of the midbrain (Fig. 6C_{ii}, 744
 745 D_{ii}). When comparing the Ox42 staining intensity 746
 747 between control side (Fig. 6A_i-G_i) and ipsilateral side 748
 749 (Fig. 6A_{ii}-G_{ii}) for the seven groups, using densitome- 750
 751 try, we measured a significant increase in the injected 752
 753 hemisphere (Fig. 6H; Side, $F_{1,33} = 22.30$, $p < 0.0001$). 754
 755 When compared to the PFFs only group, this increase 756
 757 was only significant for the h-αSyn/PFFs and h-αSyn + 758
 759 PFFs groups (*Sidak*, $p < 0.05$ and $p < 0.01$, 760
 respectively). Microglia of an amoeboid and bushy 761
 morphology, indicating a high level of activation 762
 compared to the ramified natural state, were present 763
 in high amount in animals that received both AAV- 764
 h-αSyn and PFFs, irrespective whether they were 765
 administered simultaneously or sequential (Fig. 6C_{ii}, 766
 D_{ii}, insets). This pronounced microglial activation 767
 was not detected in the control animals (Fig. 6E_{ii}- 768
 G_{ii} and H, *Sidak*, $p = n.s.$). Co-labelling of Ox42 and 769
 pSer129 (Supplementary Figure 4) showed a strong 770
 overlap between the inflammation marker and the 771
 marker for phosphorylated αSyn. 772

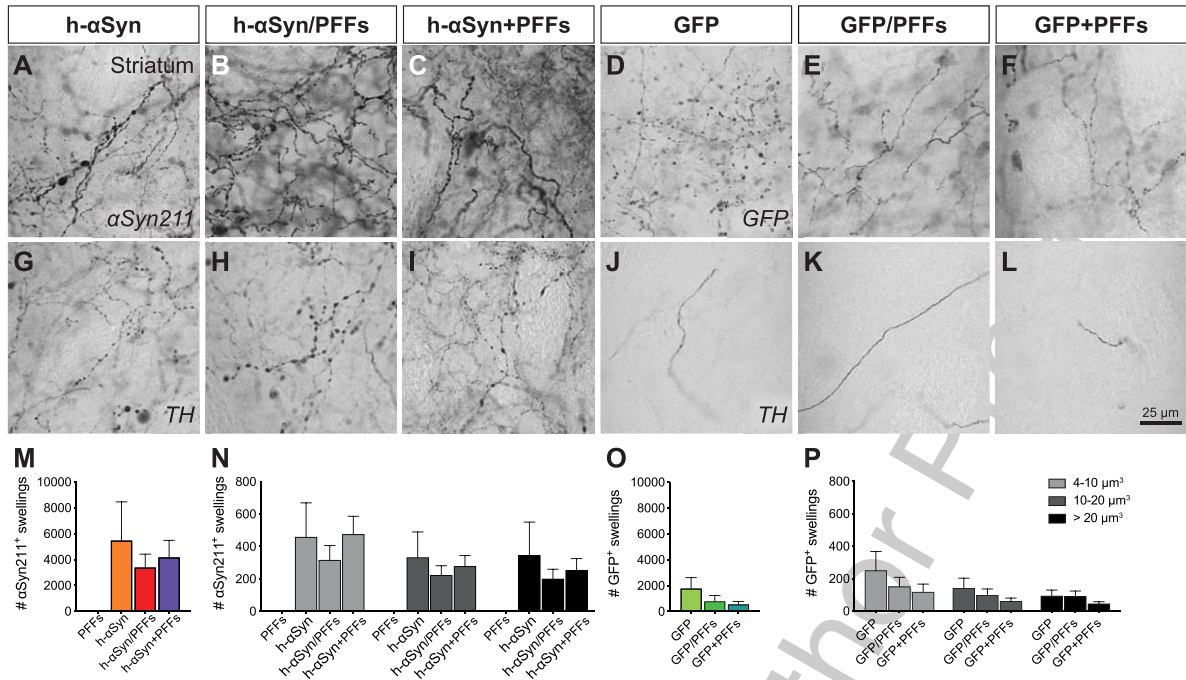


Fig. 7. Axonal pathology in the ipsilateral striatum. Immunohistochemical analysis to investigate the presence of axonal pathology using antibodies for α Syn211 (A-C), GFP (D-F), and TH (G-L). Quantification of α Syn211⁺ (M,N) and GFP⁺ swellings (O,P) in the ipsilateral striatum. The quantified swellings were counted by total number (M,O) and volume size (N,P). PFFs, preformed fibrils; h- α Syn, human alpha-synuclein; GFP, green fluorescent protein. Data are expressed as mean \pm SEM.

Axonal pathology is more pronounced in AAV-h- α Syn injected groups

The AAV injections caused a distinct dendritic pathology in the terminal fibers of midbrain dopamine neurons. In accordance with the behavioral and electrochemical data, pathological changes in striatal fibers are only seen in groups which received injections of AAV with or without additional PFFs, but not in the PFFs-only group. In high-magnification images of α Syn211 (Fig. 7A-C) and GFP (Fig. 7D-F) immunoreactivity, swellings can be detected in the three AAV groups, which are absent in the contralateral side of the brain or in PFFs-only rats (Supplementary Figure 5A-C). These swellings appear in single fibers and have a beaded chain-like structure as described previously [19]. In AAV-h- α Syn injected animals, this axonopathy could also be detected after immunohistochemistry for TH (Fig. 7G-I), while it was not detected for the AAV-GFP injected animals (Fig. 7J-L). Again, the contralateral side of the brain and PFFs only group (Supplementary Figure 5D-F) did not display any clear axonopathy.

Volumetric quantification of axonal α Syn211⁺, GFP⁺, and TH⁺ swellings further corroborated these observations. At first, we quantified the number of α Syn211⁺ and GFP⁺ swellings in target and control groups, respectively. Overall, AAV-h- α Syn injected groups had higher numbers of swellings than the AAV-GFP injected groups (Fig. 7M, O). The h- α Syn groups had 4465 \pm 1030 α Syn211⁺ swellings per brain area analyzed, while GFP control groups had 969 \pm 306 GFP⁺ swellings. As expected, PFFs only group did not show relevant numbers of α Syn211⁺ swellings (2 \pm 2). We then divided the swellings in small (5–10 μ m³), medium (10–20 μ m³), and large (>20 μ m³) volumes. Overall, the AAV-h- α Syn injected groups had higher number of swellings, independently from the size, than the AAV-GFP injected groups (Fig. 7N, P). Interestingly there was no difference in the quantity of small, medium, and large swellings within groups. Subsequently, we quantified TH⁺ swellings and obtained a proportionally similar outcome as in the previous quantification. Overall, AAV-h- α Syn injected groups had higher number of swellings than the AAV-GFP injected groups (Supplementary Figure 5G, I). Target groups had

760

761

762

763

764

765

766

767

768

769

770

771

772

773

774

775

776

777

778

779

780

781

782

783

784

785

786

787

788

789

790

791

792

793

794

795

796

797

798

799

800

801

802

803

804

805

806

807 808 ± 206 TH⁺ swellings per brain area analysed,
808 while control groups had 209 ± 124 TH⁺ swellings.
809 As above, AAV-h- α Syn injected groups had higher
810 number of TH⁺ swellings, independently from the
811 size, than the AAV-GFP injected groups (Supplemen-
812 tary Figure 5H, L) with no clear difference in the
813 quantity of small, medium, and large swellings within
814 groups.

815 These findings clearly corroborate the observed
816 functional impairments and are indicative of a stage
817 where the dopaminergic cells might be still alive, but
818 dysfunctional. As can be seen in the representative
819 images in Fig. 7, and the volumetric quantifica-
820 tions and the striatal fiber density measures reported
821 previously, the difference in the quantity of h-
822 α Syn211/GFP positive fibers and TH positive fibers
823 suggest a downregulation of TH in the striatum.

824 DISCUSSION

825 In this manuscript we present a direct comparison
826 of AAV-mediated h- α Syn overexpression and inoc-
827 ulation with PFFs either in combination or alone,
828 simultaneous or sequential. In doing so we utilized
829 human protein in a rodent background in order to
830 generate a preclinical rodent model of PD.

831 *AAV-vector based overexpression of h- α Syn*

832 AAV vectors are a preferred tool for protein over-
833 expression *in vivo* providing spatiotemporal control,
834 and they are widely used to generate preclinical
835 models for PD. AAV-based strategies have gone
836 through several generations of development, using
837 a variety of serotypes, promoters, transgenes, and
838 post-transcriptional elements. Additionally, differ-
839 ences between studies in terms of genome copies
840 (GC) injected, volumes and coordinates have intro-
841 duced a large variability in AAV-h- α Syn mediated
842 histopathological and phenotypical outcomes [11, 12,
843 66]. Overall, the overexpression of h- α Syn by AAV
844 vectors injected into the midbrain of rodents can
845 lead to a loss of TH expressing midbrain dopamine
846 cells and dopaminergic denervation of the striatum
847 [18, 19, 23, 36, 50, 67–70]. Few studies have con-
848 firmed that loss of TH immunoreactivity represents
849 overt neurodegeneration and not simply a loss of TH
850 expression [19, 67, 68, 70]. As the levels of degen-
851 eration depend on the levels of overexpressed α Syn,
852 there is a need for a vector expression system that
853 achieves robust expression and subsequent degenera-
854 tion in the majority of test subjects [19, 27]. In our
855 current study, we injected 2.4×10^{10} GC of AAV9 car-

856 rying the CBA-h- α Syn construct and animals were
857 tested over a time period of 12 weeks. We observed a
858 stable behavioral deficit, loss of TH immunoreactiv-
859 ity in midbrain and striatum, neuronal cell loss in the
860 midbrain, impaired DA release and reuptake kinet-
861 ics, as well as relevant pathology such as TH⁺ and
862 α Syn211⁺ axonal swellings. Moreover, we report the
863 development of pSer129⁺, Ub⁺, and ThioS⁺ inclu-
864 sions in midbrain indicating Lewy-like pathology.

865 *The combinatorial effect of h- α Syn and PFFs*

866 In the human condition one of the pathological
867 hallmarks of PD is the formation of Lewy bod-
868 ies and Lewy neurites in cortical and subcortical
869 structures, with one of the major components being
870 insoluble oligomers of h- α Syn assemblies [8, 71].
871 α Syn present in Lewy bodies is post-translationally
872 modified, with phosphorylation at serine 129 and
873 ubiquitination [59, 60] being among the predominant
874 modifications. Additionally, α Syn fibrils can be rec-
875 ognized by Thioflavin S dye [62]. Pre-formed fibrils
876 have been used in several model systems such as rats
877 [37, 38, 40, 42, 72] and mice [41, 73] either alone
878 or in combination with AAV-mediated overexpres-
879 sion of h- α Syn. As PFFs are cleared after injection
880 they are most frequently being injected sequentially
881 after a stable AAV-based overexpression of h- α Syn
882 has been reached for efficient seeding [37]. However,
883 more recent approaches aim for simultaneous injec-
884 tion of AAV and PFFs [40, 42], as this would negate
885 the need for a second surgery.

886 In the current study, we compare for the first time
887 the simultaneous and sequential strategies. Import-
888 antly, we did not observe significant difference
889 between h- α Syn/PFFs and h- α Syn+PFFs groups,
890 indicating that in our experimental setup the tim-
891 ing of PFFs delivery was not relevant in facilitating
892 the development of α Syn pathology. We report
893 pSer129⁺, Ub⁺, and ThioS⁺ inclusions in surviv-
894 ing midbrain neurons in all the groups injected with
895 AAV-h- α Syn and/or PFFs implying the develop-
896 ment of Lewy-like pathology. However, this was
897 especially pronounced when AAV-h- α Syn and PFFs
898 were combined, as demonstrated from the TR-FRET
899 quantification of pSer129+ α Syn aggregates in the
900 ipsilateral midbrain. These results can be explained
901 by the fact that we utilized PFFs of human origin
902 in order to better model the aggregation of this species
903 of protein. The efficiency of human PFFs in seeding
904 aggregation of endogenous rat α Syn is rather scant.
905 Our experimental paradigm thus provides for a back-
906 drop wherein one can study seeding and aggregation

of the human protein on a rat background. Whereas previous work has largely focused on rodent PFFs which alone can induce α Syn pathology and neurodegeneration in rats [38, 40, 41, 73, 74]. In agreement, our data confirmed that human PFFs alone were insufficient to trigger pathology within 12 weeks, likely due to the inability to recruit of endogenous rat α Syn. Moreover, the seeding ability is highly dependent on the levels of α Syn expressed [75] and it is thus possible that the effects of the PFFs would be more pronounced with longer incubation times in the brain. In contrast, the combination of human α Syn and human PFFs facilitated rapid templating of both endogenous and ectopic α Syn [76], thereby accelerating the pathological timeline of the AAV-vector based overexpression model. One major, albeit valid, critique of AAV vector models is that the levels of α Syn necessary to induce the levels of degeneration leading to behavioral impairments exceed those seen in patients [19]. It is important to keep this limitation in mind and critically evaluate and apply models to the specific research question [27, 77]. Another interesting difference between the h- α Syn group and the three target groups that were injected with PFFs was the difference in phosphorylated α Syn after enzymatic digestion with pK. The addition of PFFs did produce more Lewy-like insoluble α Syn aggregates whereas the pSer129⁺ inclusions were eliminated in the h- α Syn only group following pK digestion suggesting that mere h- α Syn overexpression produces a distinct aggregation species from that originating from a PFF seed.

The combination of h- α Syn and PFFs also exerted a pro-inflammatory effect. Microglia are activated by h- α Syn aggregation and may play a crucial role in PD onset and progression [78]. In pathological conditions, activated microglia migrate to the injury site where they can both exacerbate or relieve disease progression. Our data show that the combination of AAV-h- α Syn and PFFs produced a strong inflammatory response in the side of injection, where microglia had a bushy and amoeboid morphology characteristic of their activated state. This reaction might be due to the high levels of phosphorylated α Syn aggregates present in the midbrain of these animals, as demonstrated by the TR-FRET quantification.

Loss of tyrosine-hydroxylase immunoreactivity and axonal pathology

The decrease in TH is clearly indicative of changes affecting dopaminergic neurons and several studies

have shown that α Syn overexpression can lead to a downregulation of TH [27, 50, 79]. To address changes in the nigrostriatal DA system we first assessed the difference in TH immunoreactivity between the injected and the control striatum. Our data shows that h- α Syn overexpression, as well as GFP overexpression, with or without PFFs, induced a strong reduction in striatal TH immunoreactivity. This downregulation was absent only in the PFFs group. This can be indicative of TH downregulation or actual denervation. Corresponding to the striatal densitometry, unbiased stereology of TH⁺ cells in the SNpc demonstrated a loss of TH⁺ neurons ipsilateral to the injection for all the groups except the PFFs only group. A reduction in TH immunoreactivity does not causally demonstrate neurodegeneration, therefore we used double labelling for TH and the neuronal marker NeuN, confirming that the AAV-mediated overexpression does indeed lead to a loss of DA cells in the midbrain. Interestingly, the pattern of neurodegeneration appeared to spread beyond that seen with a typical 6-OHDA lesion which is specific to DA neurons.

It is important to note that the majority of preclinical rodent models of AAV vector based overexpression of α Syn has focused mainly on the loss of dopaminergic neurons alone, but axon loss and dysfunction is an early and predominant feature of PD which has been postulated to exhibit retrograde degeneration (as discussed in [80]). In the present study, AAV-h- α Syn injected animals, but not AAV-GFP injected groups, displayed an elevated number of axonal swellings in the dorsolateral striatum, the region which underlie motor function in PD.

Behavioral impairments

In humans, about 30 % of SNpc dopamine neurons and about 50–70% of striatal dopaminergic terminals are lost by the time of symptom onset [81–83]. In the present study we observed about 37% of TH loss in SNpc and 53 % in striatum of AAV-h- α Syn groups with evident dysmorphic axons, and 49% of TH loss in SNpc and 69% in striatum of AAV-GFP groups with low axonal dysmorphia. In our study, both treatment paradigms resulted in behavioral deficits, which remained stable over a period of 12 weeks. For the *d*-amphetamine induced rotations, most rats reached the behavioral threshold that is considered to be indicative of a well lesioned rat of five rotations per minute (rpm) at 8 weeks [84–86]. The threshold of 5 rpm as chosen here is considered quite

conservative as similar studies had either lower “success” rates (e.g., 25% [11]) or used a more lenient threshold of 3 rpm (e.g., [19]). It is worth also mentioning that the rotational response to d-amphetamine seen in rats is neither a naturally occurring behavior, nor does it have a linear relationship with cell loss [84, 85]. Therefore, of interest are the non-drug induced behavioral tests, where we report distinct and stable lateralized deficits in paw use on the Cylinder test (20–50% bias) and on the Stepping test (20–50% bias) for all the groups except the PFFs only group. Similar deficits have been reported on the Cylinder test when overexpressing the A53T mutant form of α Syn [23]. An interesting aspect of the AAV vector model compared to the classic neurotoxicant-based models is the fact that the behavioral impairments cannot be easily ascribed to TH-cell numbers alone. In the AAV-based model, depending on the level of transgene expression, the neuron can persist in a dysfunctional state. Many presynaptic and axonal transport proteins are indeed downregulated before overt loss of dopaminergic fibers takes place [69] and striatal dopamine levels are significantly reduced as shown by HPLC [87]. As absolute cell counts do not provide an indication of the level of functional impairment, methods such as electrochemistry are valuable additions to the characterization of the model or intervention and warrant further investigation. On the other hand, in the neurotoxicant-based models neuronal death occurs rapidly and resembles an advanced disease stage. In our study the combination of TH loss, neurodegeneration, and axonal pathology were associated with impairments in DA release- and reuptake kinetics as measured by electrochemical recordings (chronoamperometry) in the striatum. Our results suggest a direct effect of α Syn on the functionality of dopaminergic axons, which is further supported by the impaired dopamine transmission reported by us and others [50, 88, 89].

In conclusion, the pathology observed in our model is more likely caused by a combination of axonal dysfunction, TH downregulation and actual neurodegeneration. In our own work we have compared several AAV-vector constructs and observed variable behavioral and electrochemical outcomes, even though the histopathology appeared similar and in agreement with previous studies [19, 37, 90]. Importantly, we did not observe any differences between the simultaneous or sequential addition of PFFs with respect to histopathology and behavioral phenotype.

GFP as a control protein in AAV overexpression studies

GFP is a commonly used control protein in AAV overexpression-based studies. However, it has been reported that GFP can induce *in vivo* toxicity and can lead to a decrease in TH immunoreactivity [27, 28, 30]. In order to mitigate this unspecific TH loss, some studies have been lowering the titer of the AAV-GFP compared to the AAV-h- α Syn [11, 36, 91], but this approach might not be ideal in studies where protein overexpression is used to cause cell loss. The levels at which GFP vectors become toxic are not clear, and it is difficult to determine the exact gc titer in which the α Syn construct is inducing pathology while the GFP control vector has no significant effect. Albert et al. (2019) [27] reported that the GFP vector becomes significantly toxic at 3.5×10^{10} gc whereas Landeck et al. (2017) [28] set this threshold above 4×10^{11} gc. Differences in the experimental setup, vector construct and titration method do not allow for a direct comparison between studies, and it is therefore not possible to provide a precise estimate. From our own work we report neurotoxicity of h- α Syn and GFP at levels above 2.4×10^{10} gc, with minor dissimilarities between the two proteins. Differences between the present work and those reported previously may additionally come from the AAV quantification method utilized. ddPCR-based quantification is less variable than using qPCR, which can produce results varying of a factor of two or even more [92]. Therefore, in such studies where a qPCR-based quantification method was used, the actual titers might have been lower than those reported. In the present study, we injected 2.4×10^{10} gc of an AAV9 carrying the CBA-GFP construct. We observed a stable behavioral deficit, TH downregulation in mid-brain and striatum and impaired dopamine release and reuptake kinetics similarly to what observed in AAV-h- α Syn injected animals. However, AAV-GFP injected animals displayed fewer levels of axonal swellings and absence of pSer129⁺ inclusions. Our results confirm that exogenous protein overexpression can lead to unspecific neuronal pathology when it exceeds a certain threshold. The use of GFP as control protein should be taken carefully as it can complicate the interpretation of results. Alternatives such as “empty” AAVs, or AVVs carrying an inducible genome or missing the transgene might be used instead of the prototypical GFP control [27, 93, 94].

CONCLUSION

We present here a direct comparison of synucleinopathy models which result in overt dopaminergic degeneration and reliably produce a stable behavioral phenotype. Importantly, the AAV9-CBA construct utilized in our work does allow for studies to be conducted within a reasonable timeframe where neuroprotective and restorative treatments are still a viable option. However, as stated above, the levels of protein expression needed to induce a stable behavioral phenotype makes the choice of an appropriate control vector difficult. In the current study, GFP overexpression was as toxic as h- α Syn overexpression and it therefore complicated the identification of the pathological effects specific to α Syn. The transgene overexpression led to stable behavioral phenotypes, TH loss, and changes in DA kinetics. However, the presence of h- α Syn induced relevant axonal pathology, and the addition of PFFs did generate additional cell body pathology that shares some of the characteristic of human Lewy bodies. Importantly, the simultaneous injection of PFFs led to a comparable model which avoids the confounding effect of repeated injection mechanical injury of the sequential approach. This model can represent a robust platform for the study of PD related h- α Syn etiology and the development of novel targets.

ACKNOWLEDGMENTS

MD would like to thank the Royal Physiographic Society of Lund (Kungliga Fysiografiska sällskapet), the Royal Swedish Academy of Sciences (Kungliga Vetenskapsakademien) and the Per-Eric och Ulla Schybergs foundation for financial support. FPM was supported by NIH/NIDDK R01DK108798. RM and AF are supported by the EU Joint Programme on Neurodegenerative Disease Research and Agence National de la Recherche (contracts PROTEST-70, ANR-17-JPCD-0005-01 and Trans-PathND, ANR-17-JPCD-0002-02). This work has also received support from the European Union's Horizon 2020 research and innovation programme and EFPIA Innovative Medicines Initiative 2 grant agreements No 116060 (IMPRiND) and No 821522 (PD-MitoQUANT), the Swiss State Secretariat for Education, Research and Innovation (SERI) and Parkinson UK. AH would like to acknowledge generous funding by the Swedish Research Council (VR2016-01789), Demensförbundet, the

Crafoord foundation, the Gyllenstiernska Krapperupsstiftelsen, the Thorsten and Elsa Segerfalks Stiftelsen, the Åke Wibergsstiftelsen, the Kockskastiftelsen, the Royal Physiographic Society in Lund, the Swedish Parkinson Foundation (Parkinsonsfonden), the Fredrik och Ingrid Thuring's Stiftelsen, the Swedish Society of Medicine (SSMF), the Åhlenssstiftelsen, the Hedlundsstiftelsen, the Svenska Läkaresällskapet and the Jeanssonsstiftelsen.

CONFLICT OF INTEREST

The authors have no conflict of interest to report.

SUPPLEMENTARY MATERIAL

The supplementary material is available in the electronic version of this article: <https://dx.doi.org/10.3233/JPD-212555>.

REFERENCES

- Grealish S, Xie L, Kelly M, Dowd E (2008) Unilateral axonal or terminal injection of 6-hydroxydopamine causes rapid-onset nigrostriatal degeneration and contralateral motor impairments in the rat. *Brain Res Bull* **77**, 312-319.
- Kirik D, Rosenblad C, Bjorklund A (1998) Characterization of behavioral and neurodegenerative changes following partial lesions of the nigrostriatal dopamine system induced by intrastriatal 6-hydroxydopamine in the rat. *Exp Neurol* **152**, 259-277.
- Heikkila RE, Nicklas WJ, Vyas I, Duvoisin RC (1985) Dopaminergic toxicity of rotenone and the 1-methyl-4-phenylpyridinium ion after their stereotaxic administration to rats: Implication for the mechanism of 1-methyl-4-phenyl-1,2,3,6-tetrahydropyridine toxicity. *Neurosci Lett* **62**, 389-394.
- Sundstrom E, Stromberg I, Tsutsumi T, Olson L, Jonsson G (1987) Studies on the effect of 1-methyl-4-phenyl-1,2,3,6-tetrahydropyridine (MPTP) on central catecholamine neurons in C57BL/6 mice. Comparison with three other strains of mice. *Brain Res* **405**, 26-38.
- Gerhardt G, Rose G, Stromberg I, Conboy G, Olson L, Jonsson G, Hoffer B (1985) Dopaminergic neurotoxicity of 1-methyl-4-phenyl-1,2,3,6-tetrahydropyridine (MPTP) in the mouse: An *in vivo* electrochemical study. *J Pharmacol Exp Ther* **235**, 259-265.
- Ungerstedt U, Arbuthnott GW (1970) Quantitative recording of rotational behavior in rats after 6-hydroxy-dopamine lesions of the nigrostriatal dopamine system. *Brain Res* **24**, 485-493.
- Tofaris GK, Razaq A, Ghetti B, Lilley KS, Spillantini MG (2003) Ubiquitination of alpha-synuclein in Lewy bodies is a pathological event not associated with impairment of proteasome function. *J Biol Chem* **278**, 44405-44411.
- Spillantini MG, Schmidt ML, Lee VM, Trojanowski JQ, Jakes R, Goedert M (1997) Alpha-synuclein in Lewy bodies. *Nature* **388**, 839-840.

- [9] Braak H, Braak E (2000) Pathoanatomy of Parkinson's disease. *J Neurol* **247 Suppl 2**, II3-10.
- [10] Lauwers E, Debyser Z, Van Dorpe J, De Strooper B, Nuttin B, Baekelandt V (2003) Neuropathology and neurodegeneration in rodent brain induced by lentiviral vector-mediated overexpression of alpha-synuclein. *Brain Pathol* **13**, 364-372.
- [11] Kirik D, Rosenblad C, Burger C, Lundberg C, Johansen TE, Muzyczka N, Mandel RJ, Bjorklund A (2002) Parkinson-like neurodegeneration induced by targeted overexpression of alpha-synuclein in the nigrostriatal system. *J Neurosci* **22**, 2780-2791.
- [12] Klein RL, King MA, Hamby ME, Meyer EM (2002) Dopaminergic cell loss induced by human A30P alpha-synuclein gene transfer to the rat substantia nigra. *Hum Gene Ther* **13**, 605-612.
- [13] Lo Bianco C, Schneider BL, Bauer M, Sajadi A, Brice A, Iwatsubo T, Aebischer P (2004) Lentiviral vector delivery of parkin prevents dopaminergic degeneration in an alpha-synuclein rat model of Parkinson's disease. *Proc Natl Acad Sci U S A* **101**, 17510-17515.
- [14] Yamada M, Iwatsubo T, Mizuno Y, Mochizuki H (2004) Overexpression of alpha-synuclein in rat substantia nigra results in loss of dopaminergic neurons, phosphorylation of alpha-synuclein and activation of caspase-9: Resemblance to pathogenetic changes in Parkinson's disease. *J Neurochem* **91**, 451-461.
- [15] Azeredo da Silveira S, Schneider BL, Cifuentes-Diaz C, Sage D, Abbas-Terki T, Iwatsubo T, Unser M, Aebischer P (2009) Phosphorylation does not prompt, nor prevent, the formation of alpha-synuclein toxic species in a rat model of Parkinson's disease. *Hum Mol Genet* **18**, 872-887.
- [16] Gorbatyuk OS, Li S, Sullivan LF, Chen W, Kondrikova G, Manfredsson FP, Mandel RJ, Muzyczka N (2008) The phosphorylation state of Ser-129 in human alpha-synuclein determines neurodegeneration in a rat model of Parkinson disease. *Proc Natl Acad Sci U S A* **105**, 763-768.
- [17] Sanchez-Guajardo V, Febbraro F, Kirik D, Romero-Ramos M (2010) Microglia acquire distinct activation profiles depending on the degree of alpha-synuclein neuropathology in a rAAV based model of Parkinson's disease. *PLoS One* **5**, e8784.
- [18] Decressac M, Mattsson B, Bjorklund A (2012) Comparison of the behavioural and histological characteristics of the 6-OHDA and alpha-synuclein rat models of Parkinson's disease. *Exp Neurol* **235**, 306-315.
- [19] Decressac M, Mattsson B, Lundblad M, Weikop P, Bjorklund A (2012) Progressive neurodegenerative and behavioural changes induced by AAV-mediated overexpression of alpha-synuclein in midbrain dopamine neurons. *Neurobiol Dis* **45**, 939-953.
- [20] Ulusoy A, Decressac M, Kirik D, Bjorklund A (2010) Viral vector-mediated overexpression of alpha-synuclein as a progressive model of Parkinson's disease. *Prog Brain Res* **184**, 89-111.
- [21] Aldrin-Kirk P, Davidsson M, Holmqvist S, Li JY, Bjorklund T (2014) Novel AAV-based rat model of forebrain synucleinopathy shows extensive pathologies and progressive loss of cholinergic interneurons. *PLoS One* **9**, e100869.
- [22] Kanaan NM, Sellnow RC, Boye SL, Coberly B, Bennett A, Agbandje-McKenna M, Sortwell CE, Hauswirth WW, Boye SE, Manfredsson FP (2017) Rationally engineered AAV capsids improve transduction and volumetric spread in the CNS. *Mol Ther Nucleic Acids* **8**, 184-197.
- [23] Van der Perren A, Toelen J, Casteels C, Macchi F, Van Rompuy AS, Sarre S, Casadei N, Nuber S, Himmelreich U, Osorio Garcia MI, Michotte Y, D'Hooge R, Bormans G, Van Laere K, Gijsbers R, Van den Haute C, Debyser Z, Baekelandt V (2015) Longitudinal follow-up and characterization of a robust rat model for Parkinson's disease based on overexpression of alpha-synuclein with adeno-associated viral vectors. *Neurobiol Aging* **36**, 1543-1558.
- [24] Gaugler MN, Genc O, Bobela W, Mohanna S, Ardah MT, El-Agnaf OM, Cantoni M, Bensadoun JC, Sehnenburger R, Knott GW, Aebischer P, Schneider BL (2012) Nigrostriatal overabundance of alpha-synuclein leads to decreased vesicle density and deficits in dopamine release that correlate with reduced motor activity. *Acta Neuropathol* **123**, 653-669.
- [25] Landeck N, Strathearn KE, Ysselstein D, Buck K, Dutta S, Banerjee S, Lv Z, Hulleman JD, Hindupur J, Lin LK, Padalkar S, Stanciu LA, Lyubchenko YL, Kirik D, Rochet JC (2020) Two C-terminal sequence variations determine differential neurotoxicity between human and mouse alpha-synuclein. *Mol Neurodegener* **15**, 49.
- [26] Febbraro F, Sahin G, Farran A, Soares S, Jensen PH, Kirik D, Romero-Ramos M (2013) Ser129D mutant alpha-synuclein induces earlier motor dysfunction while S129A results in distinctive pathology in a rat model of Parkinson's disease. *Neurobiol Dis* **56**, 47-58.
- [27] Albert K, Vuontilainen MH, Domanskyi A, Piepponen TP, Ahola S, Tuominen RK, Richie C, Harvey BK, Airavaara M (2019) Downregulation of tyrosine hydroxylase phenotype after AAV injection above substantia nigra: Caution in experimental models of Parkinson's disease. *J Neurosci Res* **97**, 346-361.
- [28] Landeck N, Buck K, Kirik D (2017) Toxic effects of human and rodent variants of alpha-synuclein *in vivo*. *Eur J Neurosci* **45**, 536-547.
- [29] Koprlich JB, Johnston TH, Huot P, Reyes MG, Espinosa M, Broctchie JM (2011) Progressive neurodegeneration or endogenous compensation in an animal model of Parkinson's disease produced by decreasing doses of alpha-synuclein. *PLoS One* **6**, e17698.
- [30] Klein RL, Dayton RD, Leidenheimer NJ, Jansen K, Golde TE, Zweig RM (2006) Efficient neuronal gene transfer with AAV8 leads to neurotoxic levels of tau or green fluorescent proteins. *Mol Ther* **13**, 517-527.
- [31] Whone AL, Boca M, Luz M, Woolley M, Mooney L, Dharia S, Broadfoot J, Cronin D, Schroers C, Barua NU, Longpre L, Barclay CL, Boiko C, Johnson GA, Fibiger HC, Harrison R, Lewis O, Pritchard G, Howell M, Irving C, Johnson D, Kinch S, Marshall C, Lawrence AD, Blinder S, Sossi V, Stoessl AJ, Skinner P, Mohr E, Gill SS (2019) Extended treatment with glial cell line-derived neurotrophic factor in Parkinson's disease. *J Parkinsons Dis* **9**, 301-313.
- [32] Whone A, Luz M, Boca M, Woolley M, Mooney L, Dharia S, Broadfoot J, Cronin D, Schroers C, Barua NU, Longpre L, Barclay CL, Boiko C, Johnson GA, Fibiger HC, Harrison R, Lewis O, Pritchard G, Howell M, Irving C, Johnson D, Kinch S, Marshall C, Lawrence AD, Blinder S, Sossi V, Stoessl AJ, Skinner P, Mohr E, Gill SS (2019) Randomized trial of intermittent intraputamenal glial cell line-derived neurotrophic factor in Parkinson's disease. *Brain* **142**, 512-525.
- [33] Hoffer BJ, Hoffman A, Bowenkamp K, Huettl P, Hudson J, Martin D, Lin LF, Gerhardt GA (1994) Glial cell line-derived neurotrophic factor reverses toxin-induced injury

- 1339 to midbrain dopaminergic neurons *in vivo*. *Neurosci Lett*
1340 **182**, 107-111.
- 1341 [34] Wang Y, Tien LT, Lapchak PA, Hoffer BJ (1996) GDNF
1342 triggers fiber outgrowth of fetal ventral mesencephalic grafts
1343 from nigra to striatum in 6-OHDA-lesioned rats. *Cell Tissue*
1344 *Res* **286**, 225-233.
- 1345 [35] Choi-Lundberg DL, Lin Q, Chang YN, Chiang YL, Hay
1346 CM, Mohajeri H, Davidson BL, Bohn MC (1997) Dopamin-
1347 ergic neurons protected from degeneration by GDNF gene
1348 therapy. *Science* **275**, 838-841.
- 1349 [36] Decressac M, Ulusoy A, Mattsson B, Georgievska B,
1350 Romero-Ramos M, Kirik D, Bjorklund A (2011) GDNF
1351 fails to exert neuroprotection in a rat alpha-synuclein model
1352 of Parkinson's disease. *Brain* **134**, 2302-2311.
- 1353 [37] Thakur P, Breger LS, Lundblad M, Wan OW, Mattsson B,
1354 Luk KC, Lee VMY, Trojanowski JQ, Bjorklund A (2017)
1355 Modeling Parkinson's disease pathology by combination of
1356 fibril seeds and alpha-synuclein overexpression in the rat
1357 brain. *Proc Natl Acad Sci U S A* **114**, E8284-E8293.
- 1358 [38] Paumier KL, Luk KC, Manfredsson FP, Kanaan NM, Lip-
1359 ton JW, Collier TJ, Steece-Collier K, Kemp CJ, Celano
1360 S, Schulz E, Sandoval IM, Fleming S, Dirr E, Polin-
1361 ski NK, Trojanowski JQ, Lee VM, Sortwell CE (2015)
1362 Intrastratial injection of pre-formed mouse alpha-synuclein
1363 fibrils into rats triggers alpha-synuclein pathology and
1364 bilateral nigrostriatal degeneration. *Neurobiol Dis* **82**,
1365 185-199.
- 1366 [39] Volpicelli-Daley LA, Luk KC, Patel TP, Tanik SA, Rid-
1367 dle DM, Stieber A, Meaney DF, Trojanowski JQ, Lee
1368 VM (2011) Exogenous alpha-synuclein fibrils induce Lewy
1369 body pathology leading to synaptic dysfunction and neuron
1370 death. *Neuron* **72**, 57-71.
- 1371 [40] Peelaerts W, Bousset L, Van der Perren A, Moskalyuk
1372 A, Pulizzi R, Giugliano M, Van den Haute C, Melki R,
1373 Baekelandt V (2015) alpha-Synuclein strains cause distinct
1374 synucleinopathies after local and systemic administration.
1375 *Nature* **522**, 340-344.
- 1376 [41] Luk KC, Kehm V, Carroll J, Zhang B, O'Brien P, Tro-
1377 janowski JQ, Lee VM (2012) Pathological alpha-synuclein
1378 transmission initiates Parkinson-like neurodegeneration in
1379 nontransgenic mice. *Science* **338**, 949-953.
- 1380 [42] Hoban DB, Shrigley S, Mattsson B, Breger LS, Jarl U,
1381 Cardoso T, Nelander Wahlestedt J, Luk KC, Bjorklund
1382 A, Parmar M (2020) Impact of alpha-synuclein pathology
1383 on transplanted hESC-derived dopaminergic neurons in a
1384 humanized alpha-synuclein rat model of PD. *Proc Natl Acad*
1385 *Sci U S A* **117**, 15209-15220.
- 1386 [43] Bousset L, Pieri L, Ruiz-Arlandis G, Gath J, Jensen PH,
1387 Habenstein B, Madiona K, Olieric V, Böckmann A, Meier
1388 BH, Melki R (2013) Structural and functional characteriza-
1389 tion of two alpha-synuclein strains. *Nat Commun* **4**, 2575.
- 1390 [44] Sandoval IM, Kuhn NM, Manfredsson FP (2019) Multi-
1391 modal production of adeno-associated virus. *Methods Mol*
1392 *Biol* **1937**, 101-124.
- 1393 [45] Heuer A, Dunnett SB (2013) Characterisation of spatial
1394 neglect induced by unilateral 6-OHDA lesions on a choice
1395 reaction time task in rats. *Behav Brain Res* **237**, 215-222.
- 1396 [46] Ungerstedt U, Butcher LL, Butcher SG, Anden NE, Fuxe K
1397 (1969) Direct chemical stimulation of dopaminergic mech-
1398 anisms in the neostriatum of the rat. *Brain Res* **14**, 461-471.
- 1399 [47] Olsson M, Nikkhah G, Bentlage C, Bjorklund A (1995)
1400 Forelimb akinesia in the rat Parkinson model: Differen-
1401 tial effects of dopamine agonists and nigral transplants
1402 as assessed by a new stepping test. *J Neurosci* **15**, 3863-
1403 3875.
- [48] Schallert T, Norton D, Jones TA (1992) A Clinically rele-
1404 vant unilateral rat model of parkinsonian akinesia. *J Neural*
1405 *Transplant Plast* **3**, 332-333.
- [49] Schallert T, Fleming SM, Leasure JL, Tillerson JL, Bland
1406 ST (2000) CNS plasticity and assessment of forelimb senso-
1407 rimotor outcome in unilateral rat models of stroke, cortical
1408 ablation, parkinsonism and spinal cord injury. *Neurophar-*
1409 *macology* **39**, 777-787.
- [50] Lundblad M, Decressac M, Mattsson B, Bjorklund A (2012)
1410 Impaired neurotransmission caused by overexpression of
1411 alpha-synuclein in nigral dopamine neurons. *Proc Natl Acad*
1412 *Sci U S A* **109**, 3213-3219.
- [51] Hoffman AF, Gerhardt GA (1998) *In vivo* electrochemical
1413 studies of dopamine clearance in the rat substantia nigra:
1414 Effects of locally applied uptake inhibitors and unilateral
1415 6-hydroxydopamine lesions. *J Neurochem* **70**, 179-189.
- [52] Aldrin-Kirk P, Heuer A, Wang G, Mattsson B, Lundblad
1416 M, Parmar M, Bjorklund T (2016) DREADD modulation
1417 of transplanted DA neurons reveals a novel parkinsonian
1418 dyskinesia mechanism mediated by the serotonin 5-HT6
1419 receptor. *Neuron* **90**, 955-968.
- [53] Heuer A, Lelos MJ, Kelly CM, Torres EM, Dunnett
1420 SB (2013) Dopamine-rich grafts alleviate deficits in con-
1421 tralateral response space induced by extensive dopamine
1422 depletion in rats. *Exp Neurol* **247**, 485-495.
- [54] Cresto N, Gardier C, Gaillard MC, Gubinelli F, Roost P,
1423 Molina D, Josephine C, Dufour N, Auregan G, Guillemier
1424 M, Bernier S, Jan C, Gipchtein P, Hantraye P, Chartier-
1425 Harlin MC, Bonvento G, Van Camp N, Taymans JM,
1426 Cambon K, Liot G, Bemelmans AP, Brouillet E (2021)
1427 The C-terminal domain of LRRK2 with the G2019S sub-
1428 stitution increases mutant A53T alpha-synuclein toxicity in
1429 dopaminergic neurons *in vivo*. *Int J Mol Sci* **22**, 6760.
- [55] Fenyi A, Coens A, Bellande T, Melki R, Bousset L (2018)
1430 Assessment of the efficacy of different procedures that
1431 remove and disassemble alpha-synuclein, tau and A-beta
1432 fibrils from laboratory material and surfaces. *Sci Rep* **8**,
1433 10788.
- [56] Degore F, Card A, Soh S, Trinquet E, Knapik GP, Xie B
1434 (2009) HTRF: A technology tailored for drug discovery - a
1435 review of theoretical aspects and recent applications. *Curr*
1436 *Chem Genomics* **3**, 22-32.
- [57] Ip CW, Cheong D, Volkman J (2017) Stereological estima-
1437 tion of dopaminergic neuron number in the mouse substantia
1438 nigra using the optical fractionator and standard microscopy
1439 equipment. *J Vis Exp*, 56103.
- [58] Pieri L, Madiona K, Melki R (2016) Structural and func-
1440 tional properties of prefibrillar alpha-synuclein oligomers.
1441 *Sci Rep* **6**, 24526.
- [59] Fujiwara H, Hasegawa M, Dohmae N, Kawashima A,
1442 Masliah E, Goldberg MS, Shen J, Takio K, Iwatsubo T
1443 (2002) alpha-Synuclein is phosphorylated in synucleinopa-
1444 thy lesions. *Nat Cell Biol* **4**, 160-164.
- [60] Hasegawa M, Fujiwara H, Nonaka T, Wakabayashi K, Taka-
1445 hashi H, Lee VM, Trojanowski JQ, Mann D, Iwatsubo T
1446 (2002) Phosphorylated alpha-synuclein is ubiquitinated in
1447 alpha-synucleinopathy lesions. *J Biol Chem* **277**, 49071-
1448 49076.
- [61] Anderson JP, Walker DE, Goldstein JM, de Laat R, Banducci
1449 K, Caccavello RJ, Barboux R, Huang J, Kling K, Lee M,
1450 Diep L, Keim PS, Shen X, Chataway T, Schlossmacher MG,
1451 Seubert P, Schenk D, Sinha S, Gai WP, Chilcote TJ (2006)
1452 Phosphorylation of Ser-129 is the dominant pathological
1453 modification of alpha-synuclein in familial and sporadic
1454 Lewy body disease. *J Biol Chem* **281**, 29739-29752.

- [62] Huang Y, Halliday G (2013) Can we clinically diagnose dementia with Lewy bodies yet? *Transl Neurodegener* **2**, 4.
- [63] Abdelmotilib H, Maltbie T, Delic V, Liu Z, Hu X, Fraser KB, Mochle MS, Stoyka L, Anabtawi N, Krendelichtchikova V, Volpicelli-Daley LA, West A (2017) alpha-Synuclein fibril-induced inclusion spread in rats and mice correlates with dopaminergic Neurodegeneration. *Neurobiol Dis* **105**, 84-98.
- [64] Beraud D, Hathaway HA, Trecki J, Chasovskikh S, Johnson DA, Johnson JA, Federoff HJ, Shimoji M, Mhyre TR, Maguire-Zeiss KA (2013) Microglial activation and antioxidant responses induced by the Parkinson's disease protein alpha-synuclein. *J Neuroimmune Pharmacol* **8**, 94-117.
- [65] Codolo G, Plotegher N, Pozzobon T, Bruciale M, Tessari I, Bubacco L, de Bernard M (2013) Triggering of inflammasome by aggregated alpha-synuclein, an inflammatory response in synucleinopathies. *PLoS One* **8**, e55375.
- [66] Lo Bianco C, Ridet JL, Schneider BL, Deglon N, Aebischer P (2002) alpha-Synucleinopathy and selective dopaminergic neuron loss in a rat lentiviral-based model of Parkinson's disease. *Proc Natl Acad Sci U S A* **99**, 10813-10818.
- [67] Koprich JB, Johnston TH, Reyes MG, Sun X, Brotchie JM (2010) Expression of human A53T alpha-synuclein in the rat substantia nigra using a novel AAV1/2 vector produces a rapidly evolving pathology with protein aggregation, dystrophic neurite architecture and nigrostriatal degeneration with potential to model the pathology of Parkinson's disease. *Mol Neurodegener* **5**, 43.
- [68] Oliveras-Salva M, Van der Perren A, Casadei N, Stroobants S, Nuber S, D'Hooge R, Van den Haute C, Baeckelandt V (2013) rAAV2/7 vector-mediated overexpression of alpha-synuclein in mouse substantia nigra induces protein aggregation and progressive dose-dependent neurodegeneration. *Mol Neurodegener* **8**, 44.
- [69] Chung CY, Koprich JB, Siddiqi H, Isacson O (2009) Dynamic changes in presynaptic and axonal transport proteins combined with striatal neuroinflammation precede dopaminergic neuronal loss in a rat model of AAV alpha-synucleinopathy. *J Neurosci* **29**, 3365-3373.
- [70] Gombash SE, Manfredsson FP, Kemp CJ, Kuhn NC, Fleming SM, Egan AE, Grant LM, Ciucci MR, MacKeigan JP, Sortwell CE (2013) Morphological and behavioral impact of AAV2/5-mediated overexpression of human wildtype alpha-synuclein in the rat nigrostriatal system. *PLoS One* **8**, e81426.
- [71] Fares MB, Jagannath S, Lashuel HA (2021) Reverse engineering Lewy bodies: How far have we come and how far can we go? *Nat Rev Neurosci* **22**, 111-131.
- [72] Espa E, Clemensson EKH, Luk KC, Heuer A, Bjorklund T, Cenci MA (2019) Seeding of protein aggregation causes cognitive impairment in rat model of cortical synucleinopathy. *Mov Disord* **34**, 1699-1710.
- [73] Masuda-Suzukake M, Nonaka T, Hosokawa M, Oikawa T, Arai T, Akiyama H, Mann DM, Hasegawa M (2013) Prion-like spreading of pathological alpha-synuclein in brain. *Brain* **136**, 1128-1138.
- [74] Luk KC, Covell DJ, Kehm VM, Zhang B, Song IY, Byrne MD, Pitkin RM, Decker SC, Trojanowski JQ, Lee VM (2016) Molecular and biological compatibility with host alpha-synuclein influences fibril pathogenicity. *Cell Rep* **16**, 3373-3387.
- [75] Courte J, Bousset L, Boxberg YV, Villard C, Melki R, Peyrin JM (2020) The expression level of alpha-synuclein in different neuronal populations is the primary determinant of its prion-like seeding. *Sci Rep* **10**, 4895.
- [76] Giasson BI, Forman MS, Higuchi M, Golbe LI, Graves CL, Kottbauer PT, Trojanowski JQ, Lee VM (2003) Initiation and synergistic fibrillization of tau and alpha-synuclein. *Science* **300**, 636-640.
- [77] Barker RA, Bjorklund A (2020) Animal models of Parkinson's disease: Are they useful or not? *J Parkinsons Dis* **10**, 1335-1342.
- [78] Sanchez-Guajardo V, Tentillier N, Romero-Ramos M (2015) The relation between alpha-synuclein and microglia in Parkinson's disease: Recent developments. *Neuroscience* **302**, 47-58.
- [79] Perez RG, Hastings TG (2004) Could a loss of alpha-synuclein function put dopaminergic neurons at risk? *J Neurochem* **89**, 1318-1324.
- [80] Tagliaferro P, Burke RE (2016) Retrograde axonal degeneration in Parkinson disease. *J Parkinsons Dis* **6**, 1-15.
- [81] Ma SY, Roytta M, Rinne JO, Collan Y, Rinne UK (1997) Correlation between neuromorphometry in the substantia nigra and clinical features in Parkinson's disease using disector counts. *J Neurol Sci* **151**, 83-87.
- [82] Greffard S, Verny M, Bonnet AM, Beinis JY, Gallinari C, Meaume S, Piette F, Hauw JJ, Duyckaerts C (2006) Motor score of the Unified Parkinson Disease Rating Scale as a good predictor of Lewy body-associated neuronal loss in the substantia nigra. *Arch Neurol* **63**, 584-588.
- [83] Fearnley JM, Lees AJ (1991) Ageing and Parkinson's disease: Substantia nigra regional selectivity. *Brain* **114** (Pt 5), 2283-2301.
- [84] Bjorklund A, Dunnett SB (2019) The amphetamine induced rotation test: A re-assessment of its use as a tool to monitor motor impairment and functional recovery in rodent models of Parkinson's disease. *J Parkinsons Dis* **9**, 17-29.
- [85] Torres EM, Dunnett SB (2007) Amphetamine induced rotation in the assessment of lesions and grafts in the unilateral rat model of Parkinson's disease. *Eur Neuropsychopharmacol* **17**, 206-214.
- [86] Torres EM, Lane EL, Heuer A, Smith GA, Murphy E, Dunnett SB (2011) Increased efficacy of the 6-hydroxydopamine lesion of the median forebrain bundle in small rats, by modification of the stereotaxic coordinates. *J Neurosci Methods* **200**, 29-35.
- [87] Kim S, Kwon SH, Kam TI, Panicker N, Karuppagounder SS, Lee S, Lee JH, Kim WR, Kook M, Foss CA, Shen C, Lee H, Kulkarni S, Pasricha PJ, Lee G, Pomper MG, Dawson VL, Dawson TM, Ko HS (2019) Transneuronal propagation of pathologic alpha-synuclein from the gut to the brain models Parkinson's disease. *Neuron* **103**, 627-641 e627.
- [88] Hansen C, Bjorklund T, Petit GH, Lundblad M, Murmu RP, Brundin P, Li JY (2013) A novel alpha-synuclein-GFP mouse model displays progressive motor impairment, olfactory dysfunction and accumulation of alpha-synuclein-GFP. *Neurobiol Dis* **56**, 145-155.
- [89] Tozzi A, Sciacaluga M, Loffredo V, Megaro A, Ledonne A, Cardinale A, Federici M, Bellingacci L, Paciotti S, Ferrari E, La Rocca A, Martini A, Mercuri NB, Gardoni F, Picconi B, Ghiglieri V, De Leonibus E, Calabresi P (2021) Dopamine-dependent early synaptic and motor dysfunctions induced by alpha-synuclein in the nigrostriatal circuit. *Brain* **144**, 3477-3491.
- [90] Decressac M, Mattsson B, Weikop P, Lundblad M, Jakobsson J, Bjorklund A (2013) TFEB-mediated autophagy rescues midbrain dopamine neurons from alpha-synuclein toxicity. *Proc Natl Acad Sci U S A* **110**, E1817-1826.
- [91] Mulcahy P, O'Doherty A, Paucard A, O'Brien T, Kirik D, Dowd E (2012) Development and characterisation of a

- 1599 novel rat model of Parkinson's disease induced by sequen- 1611
1600 tial intranigral administration of AAV-alpha-synuclein and 1612
1601 the pesticide, rotenone. *Neuroscience* **203**, 170-179. 1613
- 1602 [92] Lock M, Alvira MR, Chen SJ, Wilson JM (2014) Absolute 1614
1603 determination of single-stranded and self-complementary 1615
1604 adeno-associated viral vector genome titers by droplet dig- 1616
1605 ital PCR. *Hum Gene Ther Methods* **25**, 115-125. 1617
- 1606 [93] Musacchio T, Rebenstorff M, Fluri F, Brotchie JM, Volk- 1611
1607 mann J, Koprach JB, Ip CW (2017) Subthalamic nucleus 1612
1608 deep brain stimulation is neuroprotective in the A53T alpha- 1613
1609 synuclein Parkinson's disease rat model. *Ann Neurol* **81**, 1614
1610 825-836. 1615
- [94] Alarcon-Aris D, Pavia-Collado R, Miquel-Rio L, Coppola- 1611
Segovia V, Ferres-Coy A, Ruiz-Bronchal E, Galofre M, 1612
Paz V, Campa L, Revilla R, Montefeltro A, Kordower 1613
JH, Vila M, Artigas F, Bortolozzi A (2020) Anti-alpha- 1614
synuclein ASO delivered to monoamine neurons prevents 1615
alpha-synuclein accumulation in a Parkinson's disease-like 1616
mouse model and in monkeys. *EBioMedicine* **59**, 102944. 1617

Uncorrected Author Proof